

Non-linear Pushover Analysis and simulation of progressive collapse mechanisms using FE Models for Nativity Church

Belal M. Almassri*¹ and Ali A. Safiyeh²

¹Civil and Architectural Engineering Department, Palestine Polytechnic University, Hebron, Palestine

²Civil Engineering Department, An-Najah National University, Nablus, Palestine

(Received October 28, 2020, Revised March 30, 2021, Accepted May 21, 2021)

Abstract. This paper presents some advanced finite element FE analyses conducted on one of the most historic structures in the world. The Church of Nativity located in Bethlehem (Palestine). To ensure the model quality, a 3D FE model was created using two different commercial software, DIANA FEA and SAP2000, one of the expected behaviors for this kind of masonry structure “low modal period” was found. The seismic behavior of the church was studied using pushover analyses, which were conducted using DIANA FEA as well as a dynamic analysis using SAP2000 is carried out using the accelerogram (1940 El Centro earthquake) to simulate a complete progressive collapse process. The first unidirectional mass proportional load pattern was created in both directions, X direction as a longitudinal direction and Y direction as the transversal direction. An incremental iterative procedure was used with monotonically increasing horizontal loads, using constant gravity loads. The results showed that the transversal direction is the most vulnerable and the damage concentrates at the main lateral (longitudinal) walls, mainly at the south and north alignment walls, and also at the vaults and at the connections of the vaults to the apse. A more accurate nonlinear dynamic analysis is recommended in the near future, which takes into account the material nonlinearity for good seismic behavior, anticipation for such an important monument, and heritage.

Keywords: DIANA FEA; FE model; masonry; non-linear analysis; SAP 2000; seismic assessment

1. Introduction

Inadequately tied masonry structures, such as monumental old buildings in urban areas, do not have enough resistance in case of strong earthquakes (Lagomarsino 2006). Natural catastrophes have always been the main reason behind the damage of cultural heritage. Masonry buildings are generally able to carry vertical loads safely but do not resist well the horizontal loads, as the masonry structures have very low tensile strength (Betti and Vignoli 2008, Lagomarsino 2006). Conducting a structural analysis of heritage masonry structure is considered complicated (Lourenço 2002, Lourenço *et al.* 2011). Some studies discussed the seismic damage and vulnerability of old historical buildings affected by earthquake activities around the world (Dogangun and Sezen 2012, Hadzima-Nyarko *et al.* 2016, Karantoni *et al.* 2014, Ranjbaran and Hosseini 2014).

There is an increasing need in the engineering society to conserve heritage buildings, there has been progressed recently in the finite element FE based numerical modeling tools, and some of these tools were adapted to be used in the analysis of masonry structures (Fajfar 2000, Magenes 2000).

A group of Byzantine towers was studied to assess their out-of-plane failure capacity and to provide seismic fragility

curves for quick estimates, the limit analysis, as well as the displacement-based methodology, were used to estimate the capacity curves of the towers, a statistical approach was adopted using the mean values and the standard deviations for the damage states with seismic intensity, and vulnerability curves were generated (Kouris *et al.* 2021). An application of image rectification to complete 2D drawings of historical buildings has been recorded by (Chalioris *et al.* 2013), the recording procedure used both the conventional topographic surveys and the photogrammetric image processing for the formation of all the façades' orthoimages.

The Pushover analysis method is a simple method used to predict the nonlinear behavior of the structure under seismic loads, it employs the lateral forces with increasing load used to push the structure until the ultimate displacement is reached, this method provides useful data about the peak response in terms of floor's displacement, story's drift, and other deformations quantities, it also can demonstrate how progressive failures in structure can occur (Reyes and Chopra 2012). The post-earthquake problems are to evaluate the most suitable strategy of retrofitting and to have enough information on the resistance of non-collapsed structures (Milani and Valente 2015a, 2015b). Both previous activities are difficult to be done because churches cannot be reduced to any standard static scheme. Recently, researchers have studied the seismic assessment and performance of historical buildings, including their details, difficulties, mechanisms, regions, and rehabilitation process. One of the important studies was done by (Lourenço *et al.* 2012) for the St James Church, using pushover analysis (Before and after the New Zealand

*Corresponding author, Assistant Professor
E-mail: mbelal@ppu.edu

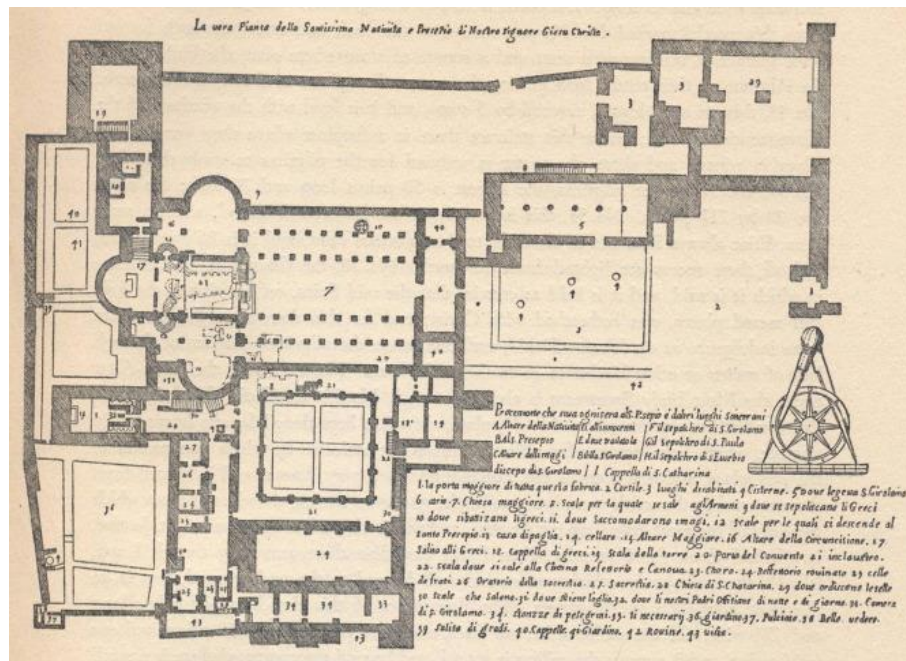


Fig. 1 Old plan of Nativity Church

Earthquake), after the nonlinear pushover analyses were carried out on both principal directions, the church was no longer safe. The analysis results of the model showed moderate agreement with the visual inspection performed in the site, which validated the model, and finally, the limit analysis using macro block analysis was also carried out to validate the main local collapse mechanisms of the church. Recently, there are many papers focused on the failure mechanisms of old masonry churches around the world, using different numerical modeling approaches, while other researchers studied the retrofitting possibilities using different approaches (Kalkbrenner *et al.* 2019, Karantoni 2013, Moratti *et al.* 2019, Noel *et al.* 2019, Ramirez *et al.* 2019, Roque *et al.* 2019, Soulis and Manos 2019, Tezcan *et al.* 2019, Tzanakis *et al.* 2016).

From the literature, many recent studies presented experimental and numerical modelling approaches considering seismic assessment for masonry buildings (Rossi *et al.* 2020, Ural 2017, Hadzima-Nyarko *et al.* 2018, Artar *et al.* 2019). Other studies focused on post-earthquake and pre-earthquake retrofitting of old reinforced concrete structures which lack sufficient flexural and shear reinforcement in columns and joints, (Tsonos 2007) studied the use of a reinforced concrete jacket and a high-strength fiber jacket for cases of post-earthquake and pre-earthquake retrofitting of columns and beam-column joints were investigated experimentally and analytically.

(Alessandri and Turrioni 2018) proposed an innovative technique for reinforcing the wall of the Nativity Church in Bethlehem against earthquakes, 3-D modal analysis of the entire church revealed that the structure is characterized by clear local modes of vibration. This showed that in the event of an earthquake, a Crusade-era wall addition is at risk of collapse via simple overturning around its base, due to the lack of firm connections with the orthogonal walls of the façade and the transept. Hence, a novel double system

of horizontal steel tension structures was designed to consolidate the wall.

Bethlehem is located between two areas of low to medium seismicity, one to the east and one to the west side. It is situated close to the fault line separating the African and Arabian tectonic plates and has been affected by several minor and major earthquakes with epicenters in the surrounding areas, such as the 1927 Palestinian earthquake, also called Jericho Earthquake. Many Palestinian cities were heavily damaged, thousands of people were left homeless, and at least 500 were estimated to be killed (Touqan and Salawdeh 2015). Strong earthquake events occurred in Palestine averagely, every one hundred years, i.e., the 1837 earthquake that occurred in the northern part of Palestine, and the 1927 earthquake, which left hundreds of victims and a lot of damage. Therefore, the engineers and researchers should focus on the vulnerability of Palestine to earthquake events. As a result, the need for this research was produced to study the architectural complex of historical structures in Palestine and to discuss its behavior against seismic vulnerability. A 3-D Finite Element model was created, a comparative modal analysis was done using both SAP 2000 and DIANA FEA to ensure the quality of the FE model, finally, a pushover analysis was conducted to investigate the phenomena of crack propagation in this masonry church.

2. Modeling of case study

2.1 Case study: The Nativity Church

The Nativity Church is one of the earliest Christian structures in the world, which is the birthplace of Jesus. The original Basilica, created in the 4th century by Emperor Constantine, which was completely damaged in the

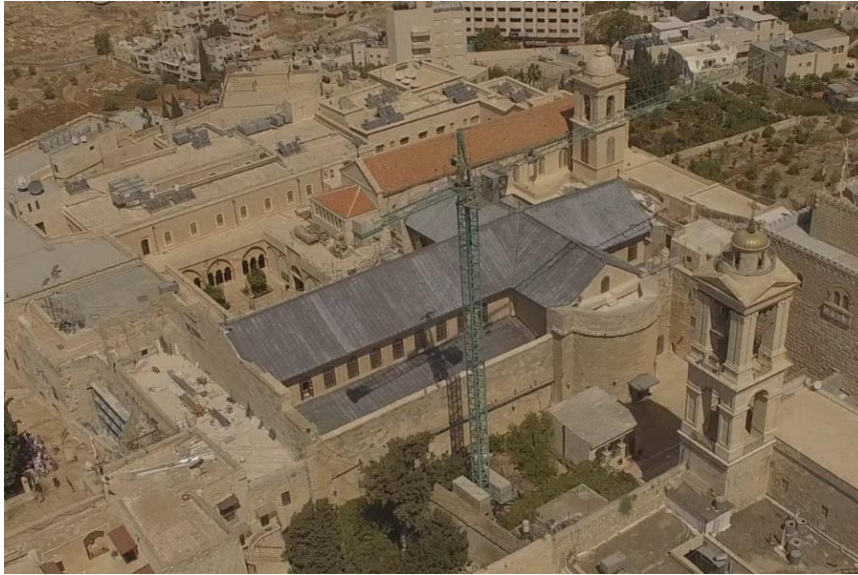


Fig. 1 Old plan of Nativity Church

Table 1 Mechanical Properties of Nativity Church

| Properties for Perimeter walls of the narthex and the Church itself | | | |
|---|----------|---------|---------|
| Fm (MPa) | td (MPa) | E (MPa) | G (MPa) |
| 4.66 | 0.089 | 1429 | 460.75 |
| Properties for some specific narthex components | | | |
| Fm (MPa) | td (MPa) | E (MPa) | G (MPa) |
| 3.49 | 0.067 | 868.38 | 147.25 |
| Properties for vaults | | | |
| Fm (MPa) | td (MPa) | E (MPa) | G (MPa) |
| 1.01 | 0.02 | 456.75 | 147.25 |

Samaritan Revolt (Shomali 2003). Fig. 1 shows an old plan of the church which was drawn by Fr. Bernardino Amico in 1609 (Milani *et al.* 2016).

It was replaced later on the same site, by another basilica; which was different in its plan and had at that time, modified parts of the original building (Shomali 2003), fig. 2 presents the current basilica, which is located in Bethlehem, over a fertile limestone hill, the figure gives a visualization of the whole structure of the church, its mainly constructed of masonry walls, which are composite material consisting of an assemblage of stones and mortar joints, each of them has different properties, and due to the low tensile and shear bond strength, mortar joints act as a plane of weakness.

2.2 Mechanical properties

The Nativity Church was restored and some components rebuilt again many times, so it has different materials which can be noticed through visual inspection, but it is difficult to use in-situ inspection techniques such as coring, flat jack test, sonic tomography, thermo vision, etc. due to privacy and saintliness. The mechanical properties of the materials used in the numerical model will be used based on onsite tests, which have been carried out by (Alessandri and Turrioni 2018). These tests focused on the structural

components of the Church and the material properties of masonry walls like compressive strength (Fm), shear strength (td), Young's modulus (E), shear modulus (G), Poisson coefficient (ν), and self-weight (w). Table 1 summarizes these values for the components of the church as published before. On the other hand, the assumptions used in this paper refer to that masonry structures have very low tensile strength, so in the analysis, the tensile strength is assumed 5% of the compression strength. In more detail, for narthex and church walls, the tensile strength is 0.233 mPa, for some specific narthex components, 0.175 MPa, and 0.05 MPa for the vaults.

3. FE numerical modeling

3.1 Software's used

Through the study of SAP2000 and DIANA FEA software's which are used in the analysis, important highlights can be shown, in the first hand; SAP2000 is a finite element package used mainly by civil engineers, which can analyse general structures, i.e., buildings, bridges, dams, and solids, etc. but, in the second hand, DIANA FEA is advanced finite element software usually used for advanced works and simulations, also mainly in

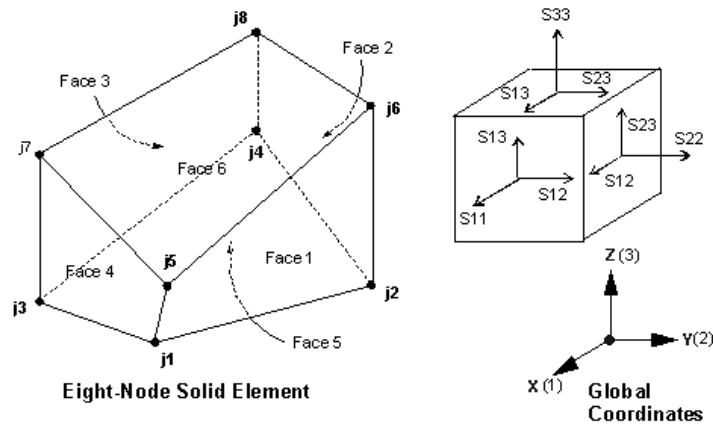


Fig. 3 Eight node solid element in SAP2000

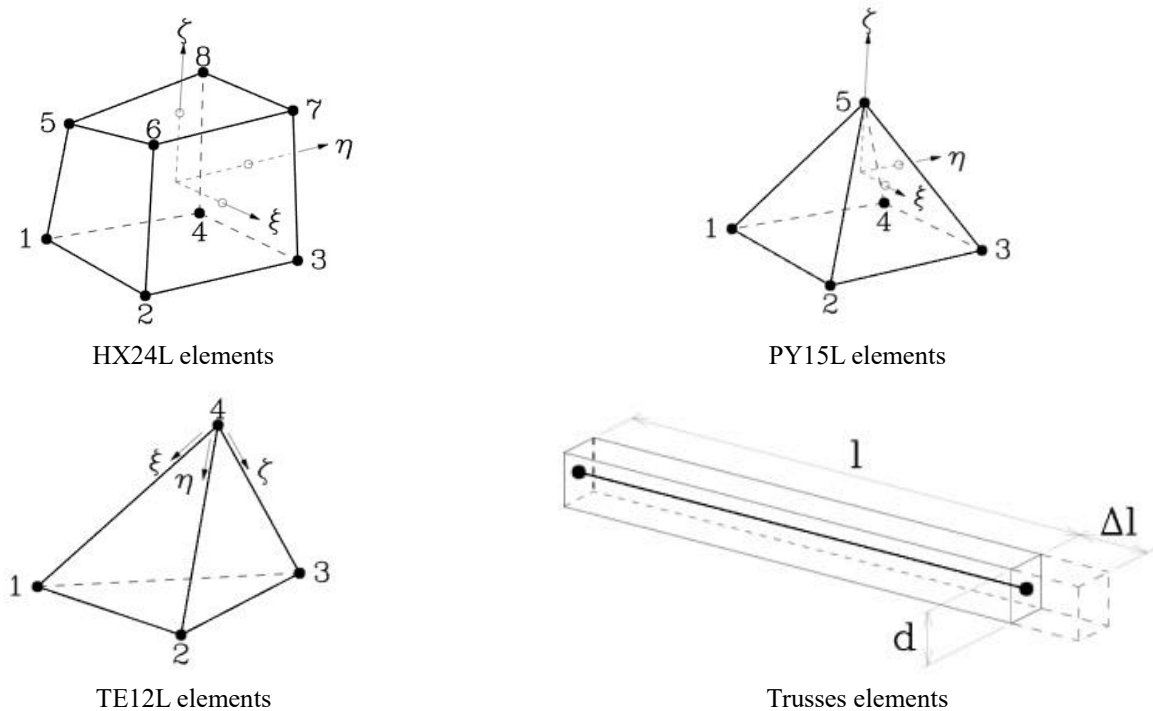


Fig. 4 3D Solids used in modeling according to DIANA manual

academic purposes. In detail; the physical problems concerning fluids flow, heating, contact analysis, also, static and dynamic analysis can be simulated by DIANA FEA easily.

The solid element used by SAP2000 is an eight node; each solid element has six quadrilateral faces, with a joint located at each of the eight corners as shown in Fig. 3, in addition, the solid elements of SAP2000 have three translational degrees of freedom at each joint, and the rotational degrees of freedom are not active. The stresses are evaluated by using the standard Gauss integration points of the elements and extrapolated to the joints.

On other hand, DIANA FEA, gives numerous kinds of solid elements, the type of regular solid elements used for the numerical model, according to the DIANA FEA manual, are; firstly, HX24L element, which is a brick geometric

element with eight nodes, Fig. 4(a), and establish about 17280 units in the model. Secondly, the PY15L element which is a pyramid geometric element with 5 nodes, 4 sides, and found in 238 location in the model, Fig. 4(b), thirdly, there are 624 units of TE12L element, Fig. 4(c), which is characterized as tetrahedron geometric element with 4 nodes and 3 sides, and in the final, the trusses elements in the model, are modelled as bars which meet the condition that the dimension D perpendicular to the bar axis is small to the bar's length L , as Fig. 4(d) and exist in 47 location as 480 units.

The tetrahedral elements can fit better the complex geometry; although when it is used to integrate the shape functions with points of Gauss it is less accurate than hexahedral elements.

In addition, one of the factors that determine the quality

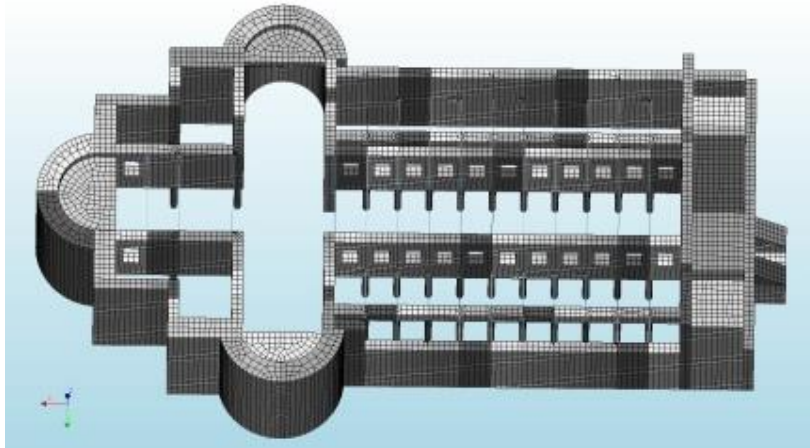


Fig. 5 0.50 m mesh for the model

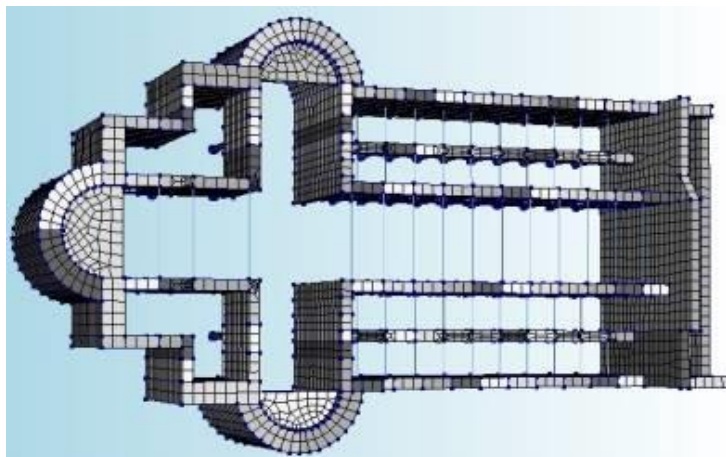


Fig. 6 0.35 m mesh for the model

Table 2 Meshing sensitivity study results

| Mesh Size | X – Direction (In-plane) | Y – Direction (Out-of- Plane) |
|-----------|--------------------------|-------------------------------|
| | Maximum Crack width | Maximum Crack width |
| 100 cm | 0.56 mm | 1.12 mm |
| 85 cm | 1.02 mm | 3.34 mm |
| 50 cm | 3.24 mm | 13.7 mm |
| 35 cm | 3.24 mm | 13.7 mm |

of the mesh is the distortion of its elements. The reason for these lays in the mapping from real to natural space of integration, but for the same degree of the polynomial, the finite element space generated by hexahedral elements is richer than the space generated by tetrahedral elements. However, the tetrahedral elements as mentioned previously are best to model complex geometry domain with little distortion of mesh, and also the computational cost for assembling the global stiffness matrix for tetrahedral elements is lower because there is not necessarily numerical integration.

The meshed model consists of more than 18500 elements, the software adopted to investigate the modal characteristics of the structures. The refined mesh applying a sensitivity analysis was carried out with elements equal 0.5 m side for the church, much finer than this, took much time in the analysis procedure and can make remarkable

divergence for the analysis to give logical results while coarser than 0.5 m did not present remarkable cracks width in the two directions as shown in Table 2, which presents the cracks width versus meshing size in both directions, Figs. 5 and 6 show two different gradients in meshing procedure.

As shown in Table 2, the mesh size used 0.5 m, was the used one for the church, there were no remarkable increases in maximum crack width in both directions if finer mesh size was implemented, it is clear that the crack width increases if the mesh size was decreases till 0.5 m side as shown in the previous table.

3.2 Modal Analysis

In this section, the investigation of modal analysis will be done to show the vulnerability and possibility for out-of-

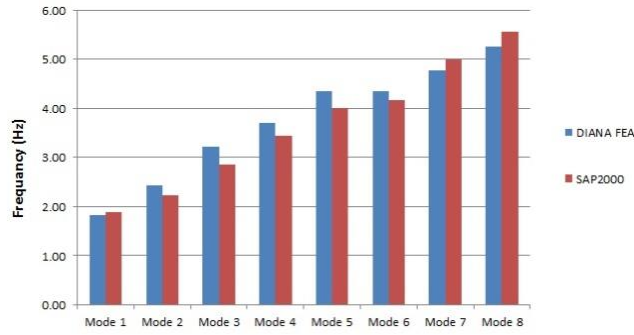


Fig. 7 Frequencies for the two models

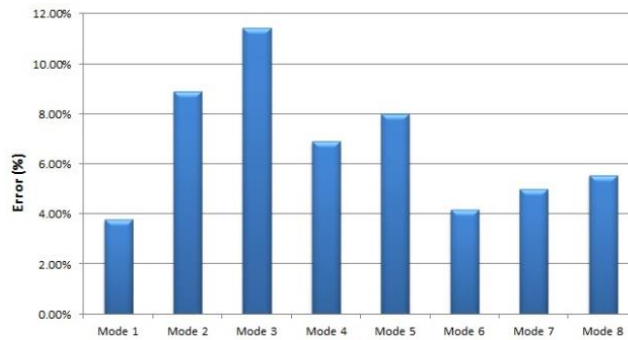


Fig. 8 Errors % for the two models

Table 3 Modal Analysis Using SAP 2000 and DIANA FEA

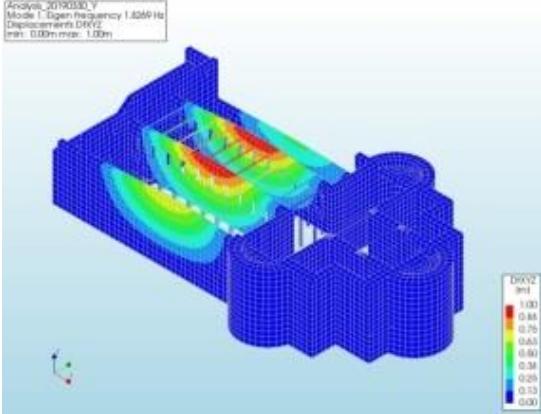
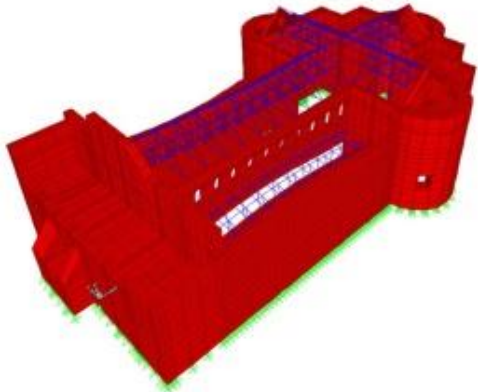
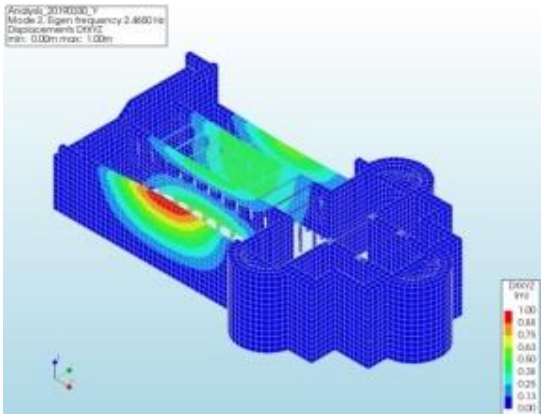
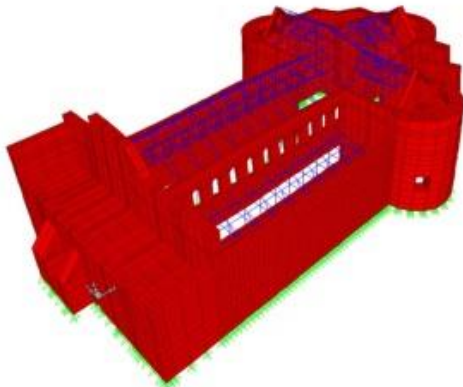
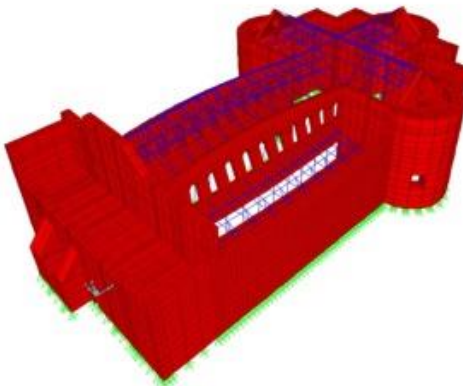
| SAP 2000 Model | DIANA FEA Model |
|---|--|
|  <p>Mode (1) T=0.53 sec, F=1.89 Hz</p> |  <p>Mode (1) T=0.55 sec, F=1.83 Hz</p> |
|  <p>Mode (2) T=0.45 sec, F=2.22 Hz</p> |  <p>Mode (2) T=0.41 sec, F=2.47 Hz</p> |

Table 3 Continued



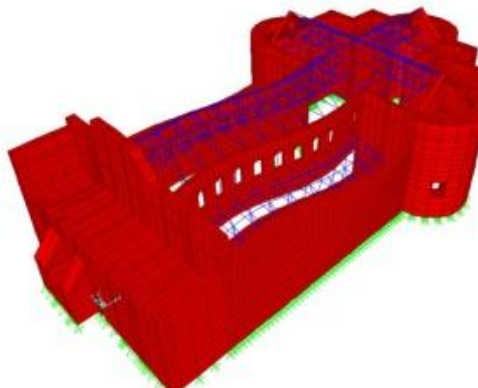
Mode (3) T=0.35 sec, F=2.86 Hz



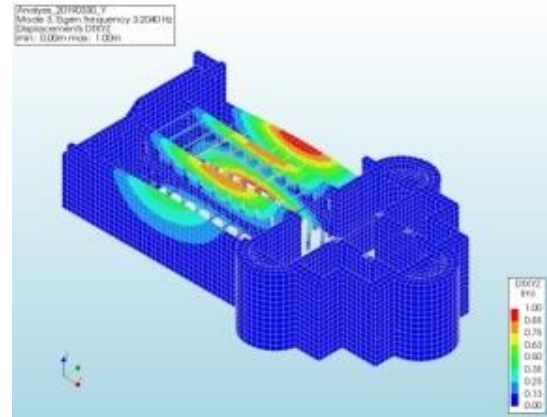
Mode (4) T=0.29 sec, F=3.45 Hz



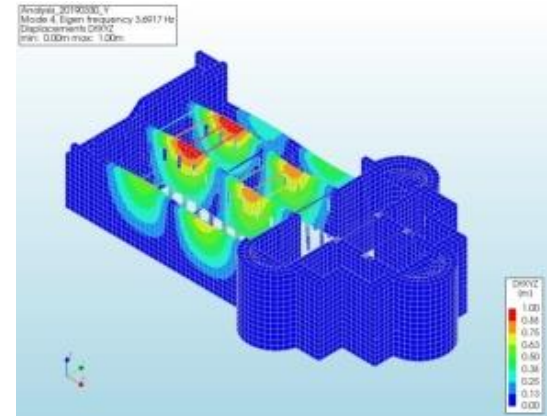
Mode (5) T=0.25 sec, F=4.00 Hz



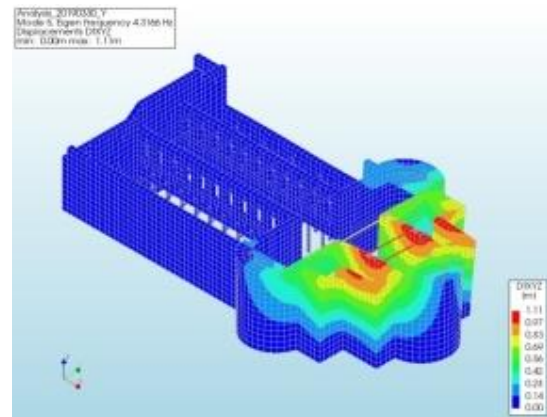
Mode (6) T=0.24 sec, F=4.17 Hz



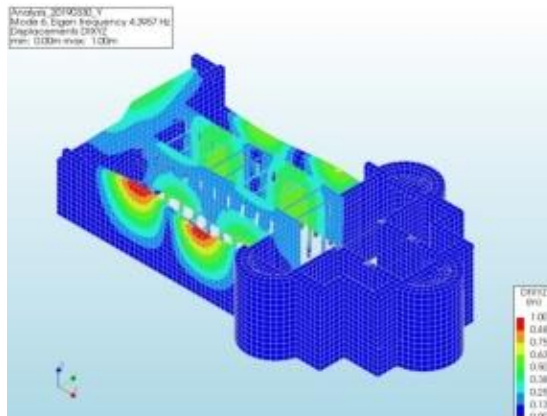
Mode (3) T=0.31 sec, F=3.20 Hz



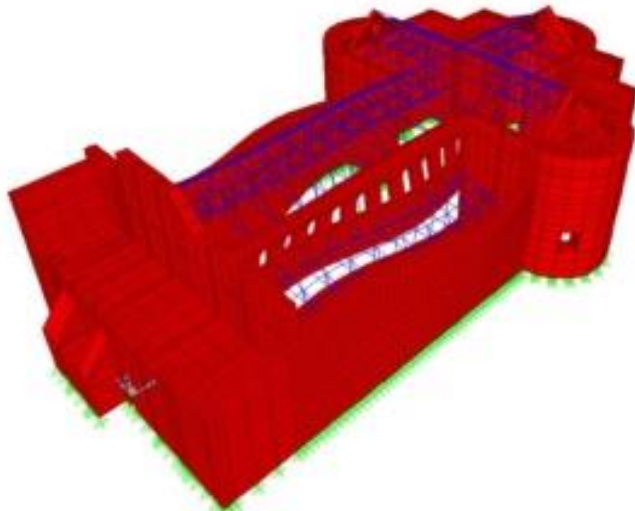
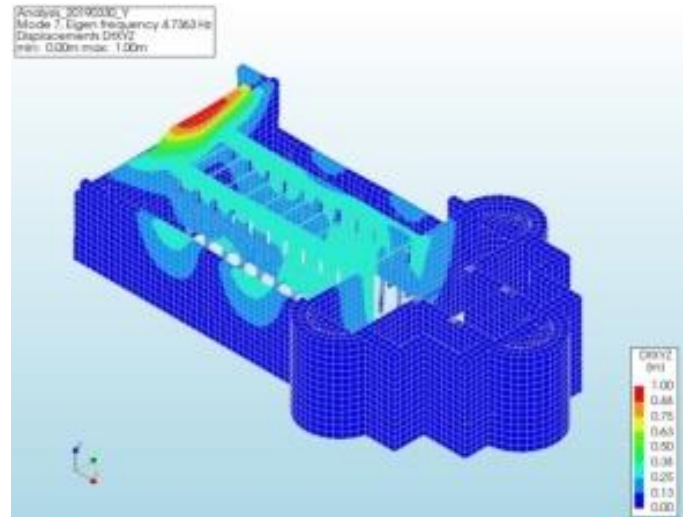
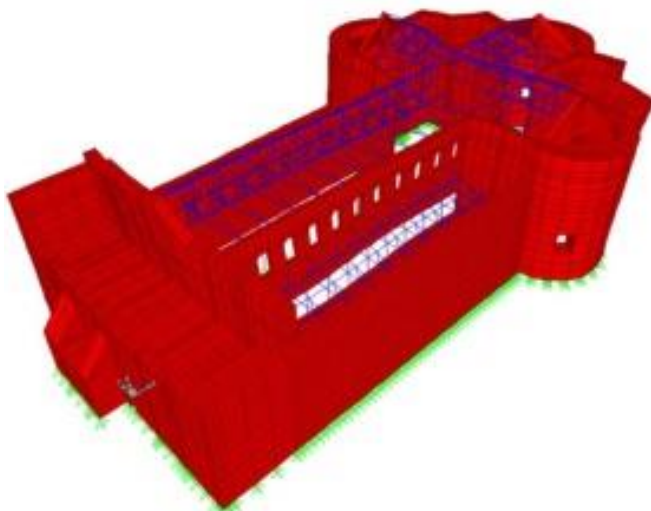
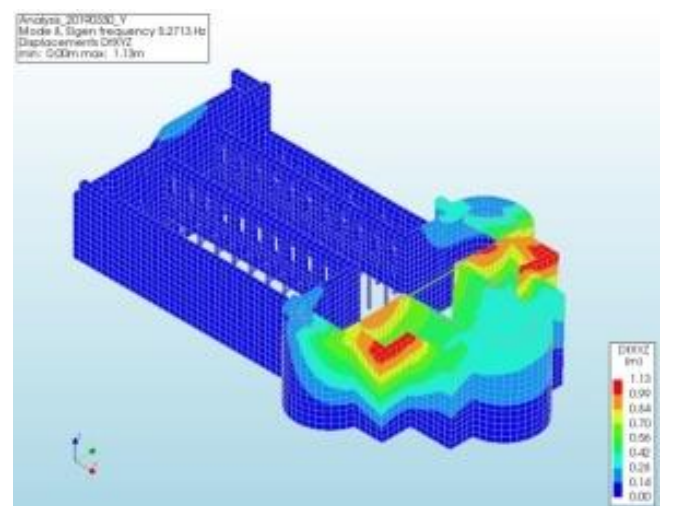
Mode (4) T=0.27 sec, F=3.69 Hz



Mode (5) T=0.23 sec, F=4.32 Hz



Mode (6) T=0.23 sec, F=4.40 Hz

Mode (7) $T=0.20$ sec, $F=5.00$ HzMode (7) $T=0.21$ sec, $F=4.74$ HzMode (8) $T=0.18$ sec, $F=5.56$ HzMode (8) $T=0.19$ sec, $F=5.27$ Hz

plane mechanisms. Table 3 shows the corresponding modal periods for the first 8 modes, generated from SAP 2000 and DIANA FEA and followed by a comparison between them for verification. In detail, the first, fourth, and sixth modes show the applicability of the interior walls to overturn and move in harmonically motion. In addition, out-of-plane mechanisms are possible also for the southern and northern walls, whose safety assessment would be necessary for local analysis, and can be confirmed in the second and third modes. As similar, the five and eight modes of the “as it is” model involves the translation motion in the two principal directions of church shoulders, these shoulders which have the properties of perimeter walls, play an important role in the connections between semi-circular apses, and finally, the seventh mode shows the overturning mechanism of façade, which undergoes larger displacement.

Figs. 7 and 8 show the modal frequencies and the errors corresponding to the modal periods, respectively, after the assumption of DIANA FEA results as more accurate. It's obvious that the modal periods are very close to each other

and the maximum percentage error is 11.23%.

3.2 Pushover Analysis using DIANA FEA

The material model which was used for the behaviour of the masonry structure consists of two models which are the smeared cracking model for tension and the plasticity model for compression, as shown in Fig. 9 which presents final inelastic stress-strain relationships adopted in the constitutive model of the church for both the walls and the vaults. The smeared crack approach was generated directly from the computational of continuum mechanics. This means that the criteria of cracks propagations and, eventually, the prediction of the direction of propagation came directly from this theory, so, mostly, based on failure criteria expressed in terms of stresses or strains. It's important to say that smeared crack models do not account for discontinuities in the topology of the finite element mesh, so re-meshing is unnecessary. The linear tension softening based on the energy of the fracture which was

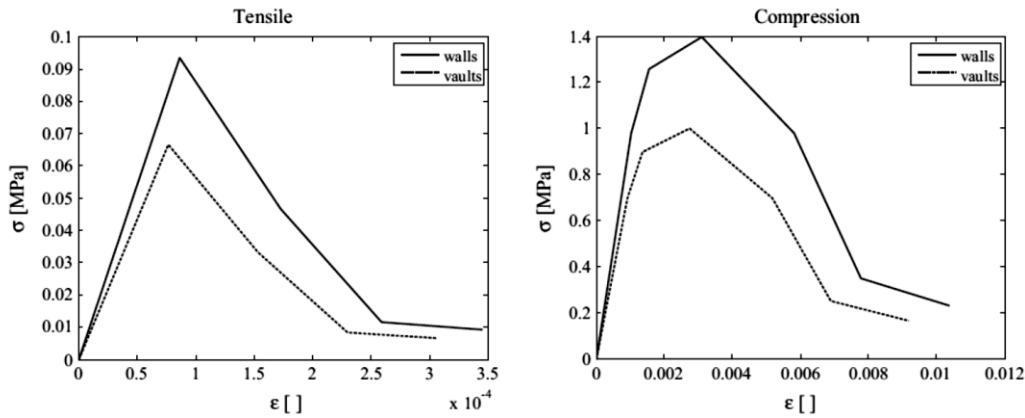


Fig. 9 Material constitutive models used for masonry behavior

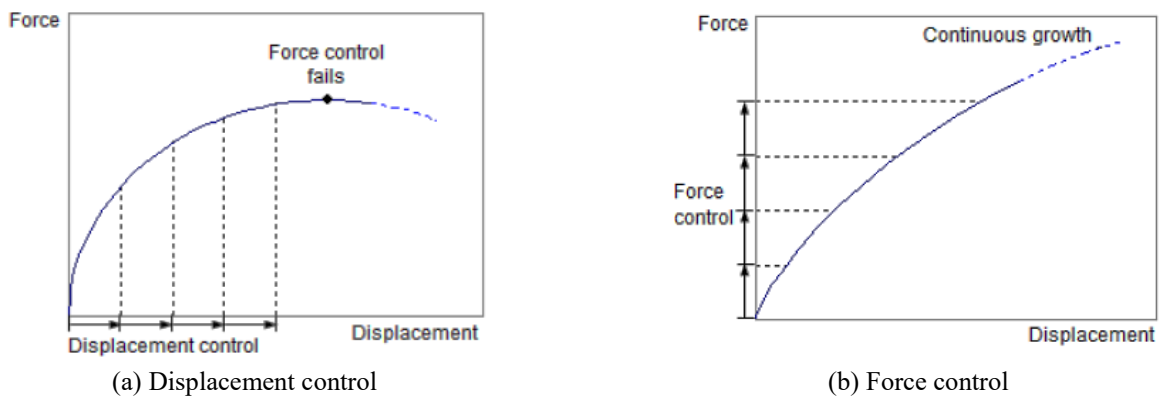


Fig. 10 Displacement control versus force control (Palacio 2013)

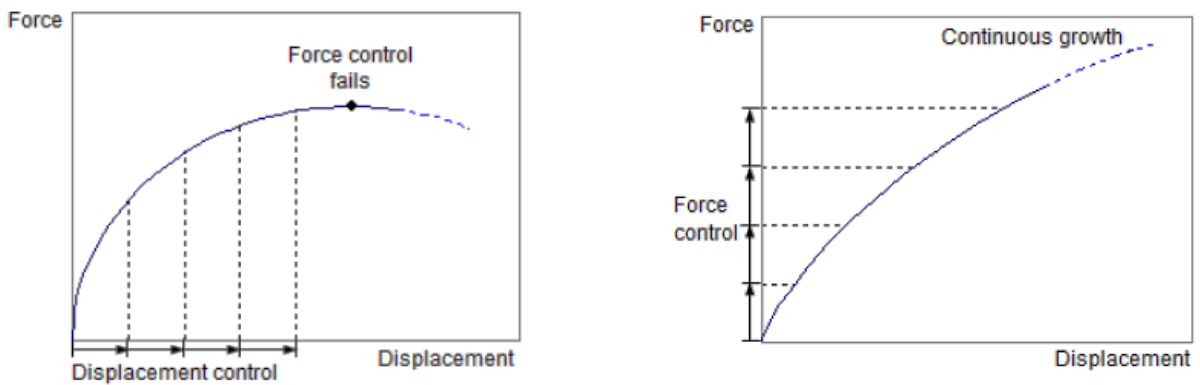


Fig. 11 Load increment methods characteristics and arc-length control (Palacio 2013)

selected, and the crack bandwidth was used, the cracks continuously spread within the element, and the stiffness was reduced, finally, a constant shear retention factor is chosen due to the cracking of the material.

For the entire aforementioned pushover analyses, the regular Newton-Raphson method was used for the iteration process, an energy convergence control with a tolerance of 10^6 . In displacement control analysis, the displacement of a reference point is incrementally applied, but in force control method, and for the models experiencing softening, this method cannot lead to a solution when the load applied is higher than the capacity, Fig. 10 shows the two procedures:

The arch length should be taken into account, as the

load-displacement curve is almost horizontal, the prediction of the displacements' increment is large, and when the loads' increment is fixed, the results of displacements will be also large. The analysts use arc-length control, where the increment is adjusted, and this method is illustrated in Fig. 11.

The iterative process was defined by DIANA FEA. Adapted iteratively by the increment until equilibrium is achieved. The total displacement of the iteration is therefore defined as

$$\Delta_{ui+1} = \Delta_{ui} + \sigma_{ui+1} \quad (1)$$

Where Δ_{ui+1} represents the total displacement increment

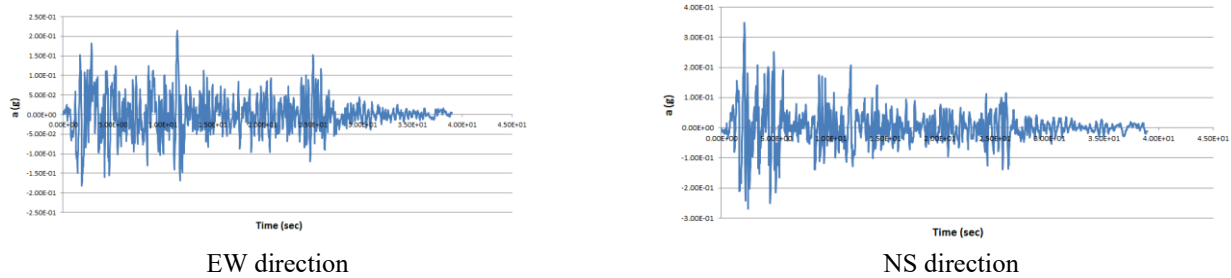


Fig. 12 Accelerogram of El Centro Earthquake

at iteration (i), Δ_{ui} is the total displacement increment at iteration (i+1), and δ_{ui+1} is the iterative increment.

3.3 Progressive Collapse Analysis using SAP2000

To prevent the collapse of valuable and historical buildings, it is necessary to fully understand their failure mechanisms and to improve safe earthquake excitations period by focusing on critical regions of the structure, as the masonry structures present substantial vulnerability to rock falls, with scarce methodologies for the damage quantification of structures subjected to rock falls, an analytical procedure for the damage assessment of masonry structures is presented in this section. The procedure starts with applying the dynamic analysis with real earthquake accelerogram to the model, the second step is adapting failure criterion to masonries (Von Misses) to gain results from analysis which was applied, then comparing the results to the limit state values as ultimate shear stresses for each component, and finally, localizing the critical and collapsed regions in the model and determine the exact time of this failure during the analysis.

The analysis is carried out with the finite element program SAP2000 on the model of Nativity Church. In details, the dynamic analysis is carried out using the accelerogram regards the 1940 El Centro earthquake which was occurred at 21:35 Pacific Standard Time on May 18 (05:35 UTC on May 19) in Southern California near the international border of the United States and Mexico, shown in Fig. 12. This earthquake had a magnitude of 6.9 on the Mercalli intensity scale and was the first major earthquake to be recorded by a strong-motion seismograph located next to a fault rupture, (Trifunac, M.D.; Brune, J.N.).

In this section, the applied accelerogram lasts 39.00 seconds and all information is obtained from the U.S. Geological Survey website (USGS.GOV). Subsequently, the principal stresses distributions over the model are shown, also the Von Misses stress are calculated for each time step. The scale mathematical formula used to determine the seismicity of location with amplitude and distance is shown in Eq. (2)

$$\text{Scaling Factor} = (I * Z) / (Z1 * R) \quad (2)$$

- I: Importance factor,
- Z: Seismic Zone Factor of Bethlehem, (0.15 g), according to Seismic Hazard Map
- Z1: Amplitude for chosen earthquake,

- R: inelastic factor.

3.3.1 Critical region identification

The main objective of this section is to identify the critical and vulnerable regions of stone components considering the church, collapses are often caused by defects or damages at the critical regions during the service stage. The church of Nativity consists of a series of components; each of them has a different degree of importance subjected to external loads. To ensure global integrity and safety, the critical components and regions should be given greater safety margins.

The basic concept behind the determination of the critical components and regions is to strengthen these structural elements, so the building turn into the phase to be capable of resisting a specific level of threat, which may be in the form of blast, impact or any other abnormal event coming from this “key” elements. The limits of allowable progressive collapse as given in many design codes and guidelines are slightly different. For example, UK building regulations require the key elements to be designed for resisting an abnormal load of 34 KN/m² applied in any direction.

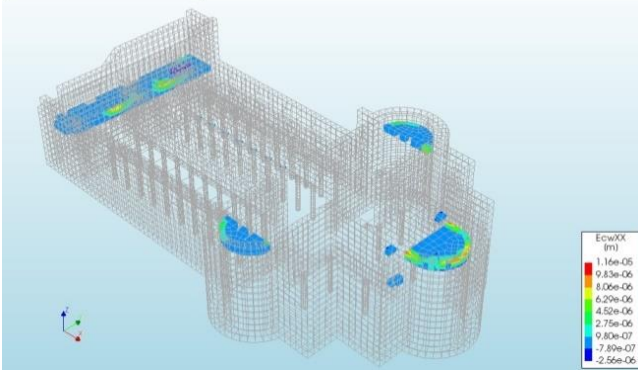
4. Results and Discussion

The results are reported in terms of crack propagation, as the main goal of this study is to investigate the phenomena of crack initiation in masonry structures during an earthquake activity, so the FE model was constructed using DIANA FEA, using the pushover analysis. This analysis method is usually used to appreciate the seismic performance of masonry structures by making a simulation using static horizontal forces. A complete progressive-collapse process was also generated using SAP2000, to find with according to Von Misses results the Critical Region Identification. Moreover, the material exhibits a nonlinear behaviour, by which the cracking pattern can be generated. The results present crack propagation in the whole church in both directions X and Y, which helps in understanding the general failure pattern.

4.1 Cracks in X – Direction

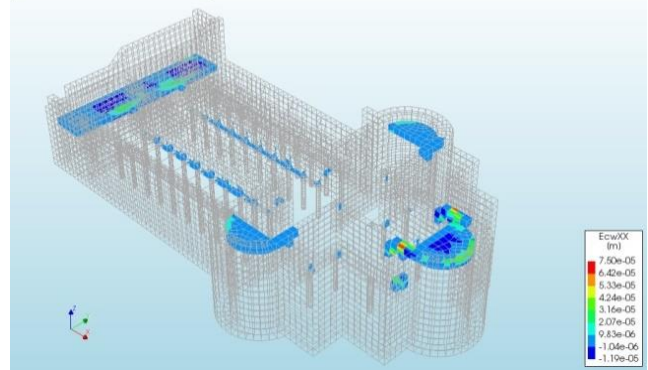
The analysis of the Nativity Church determines the critical elements by monitoring the crack propagation in each element, i.e., some church elements often present

Analysis_20190330_X
Load-step 1, Load-factor 0.19961, Self Load
Crack-widths EcwXX
min: -2.36e-06m max: 1.16e-05m



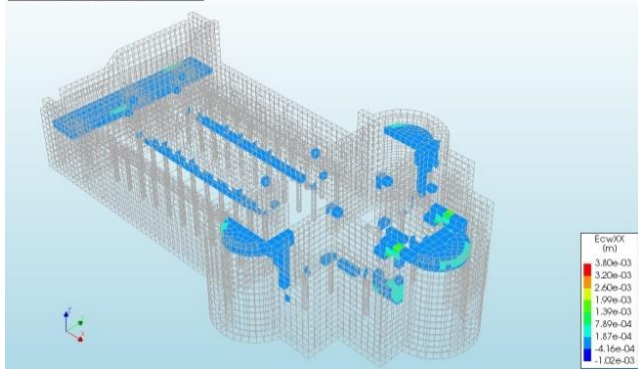
Load Step (1) : Crack width 0.012 mm

Analysis_20190330_X
Load-step 2, Load-factor 0.39656, Self Load
Crack-widths EcwXX
min: -1.19e-05m max: 7.50e-05m



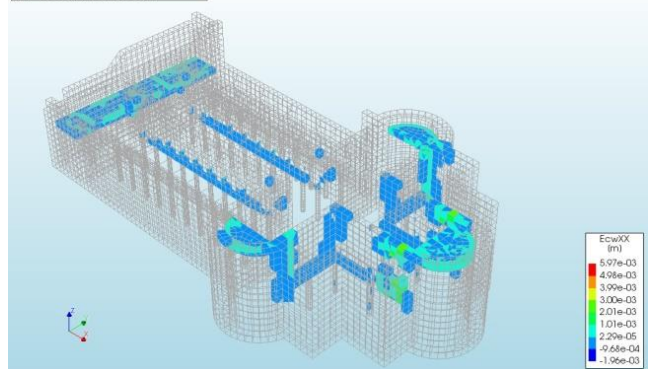
Load Step (2) : Crack width 0.075 mm

Analysis_20190330_X
Load-step 3, Load-factor 0.48763, Self Load
Crack-widths EcwXX
min: -1.02e-03m max: 3.80e-03m



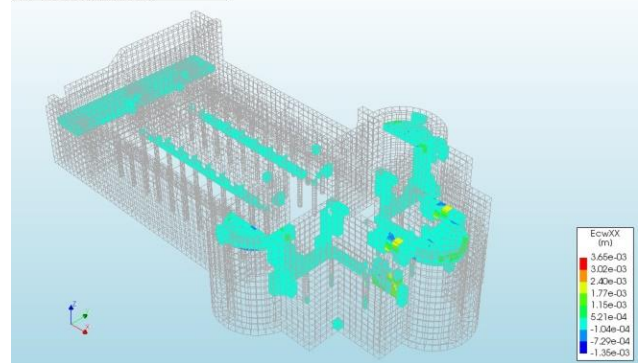
Load Step (3) : Crack width 3.80 mm

Analysis_20190330_X
Load-step 4, Load-factor 0.11686, Self Load
Crack-widths EcwXX
min: -1.95e-03m max: 5.97e-03m



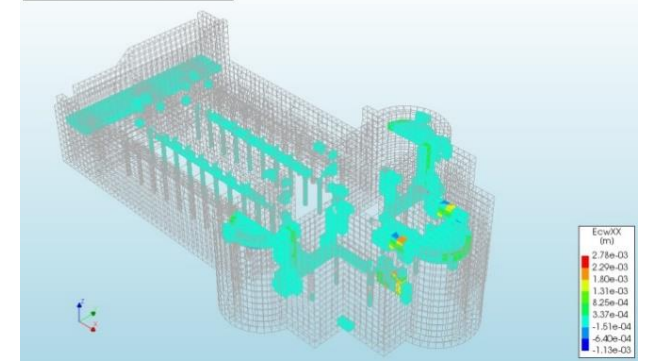
Load Step (4) : Crack width 5.97 mm

Analysis_20190330_X
Load-step 5, Load-factor -0.14698E+01, Self Load
Crack-widths EcwXX
min: -1.35e-03m max: 3.65e-03m



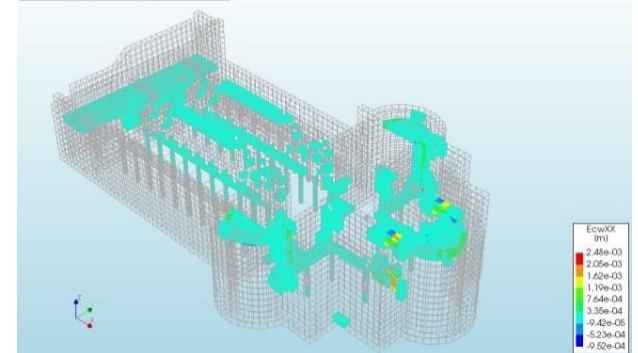
Load Step (5) : Crack width 3.65 mm

Analysis_20190330_X
Load-step 6, Load-factor -0.77710E+01, Self Load
Crack-widths EcwXX
min: -1.13e-03m max: 2.78e-03m



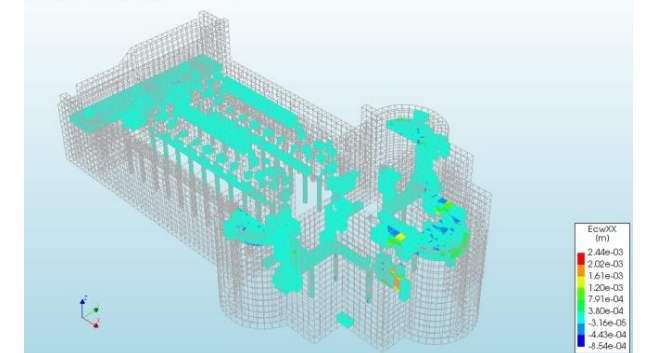
Load Step (6) : Crack width 2.78 mm

Analysis_20190330_X
Load-step 7, Load-factor -0.93976E+01, Self Load
Crack-widths EcwXX
min: -0.52e-04m max: 2.48e-03m



Load Step (7) : Crack width 2.48 mm

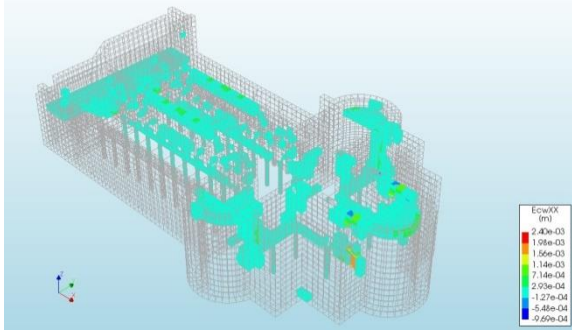
Analysis_20190330_X
Load-step 8, Load-factor -0.95650E+01, Self Load
Crack-widths EcwXX
min: -5.54e-04m max: 2.44e-03m



Load Step (8) : Crack width 2.44 mm

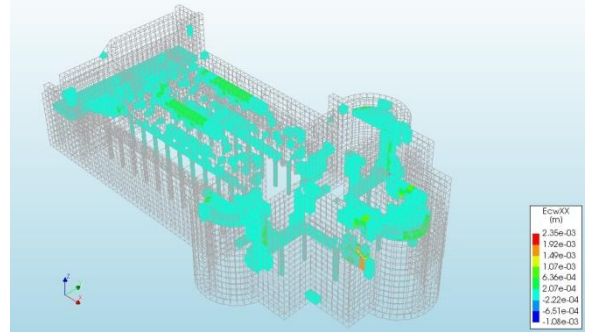
Fig. 13 Continued

Analysis_20190330_X
Load-step 9, Load-factor 0.9209E-01, Self Load
Crack-widths EcwXX
min: -9.26e-04m max: 2.40e-03m



Load Step (9) : Crack width 2.40 mm

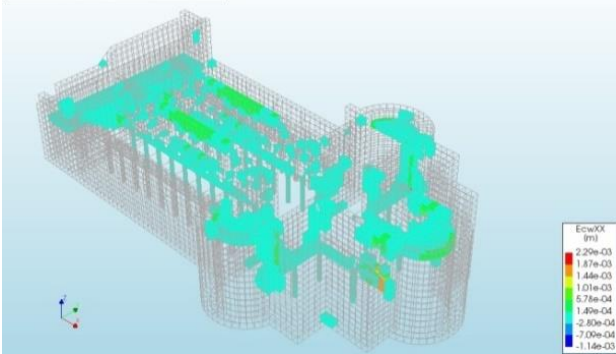
Analysis_20190330_X
Load-step 10, Load-factor 0.8909E-01, Self Load
Crack-widths EcwXX
min: -1.03e-03m max: 2.35e-03m



Load Step (10) : Crack width 2.35 mm

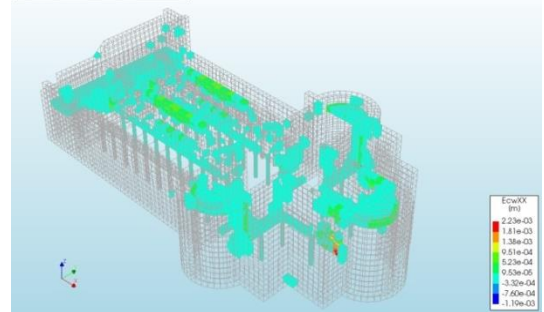
Fig. 13 Crack widths generated by gravity loads analysis in X – direction

Analysis_20190330_X
Load-step 11, Load-factor 0.80125E-01, Pushover_X
Crack-widths EcwXX
min: -1.14e-03m max: 2.29e-03m



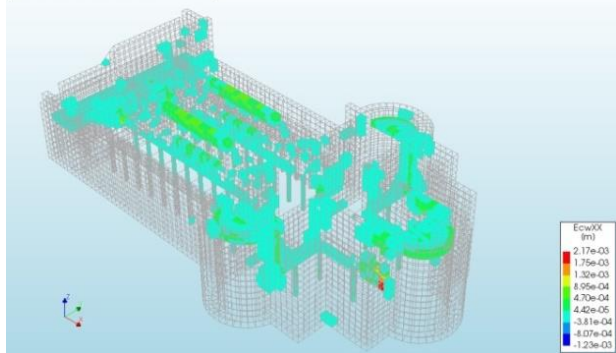
Load Step (11) : Crack width 2.29 mm

Analysis_20190330_X
Load-step 12, Load-factor 0.19255, Pushover_X
Crack-widths EcwXX
min: -1.19e-03m max: 2.23e-03m



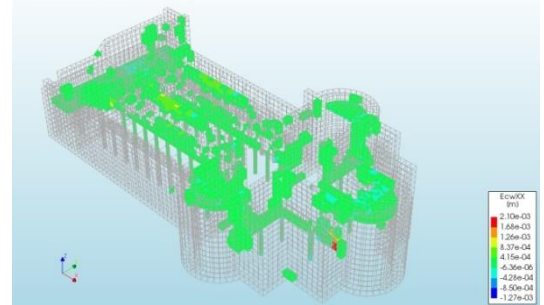
Load Step (12) : Crack width 2.23 mm

Analysis_20190330_X
Load-step 13, Load-factor 0.20443, Pushover_X
Crack-widths EcwXX
min: -1.23e-03m max: 2.17e-03m



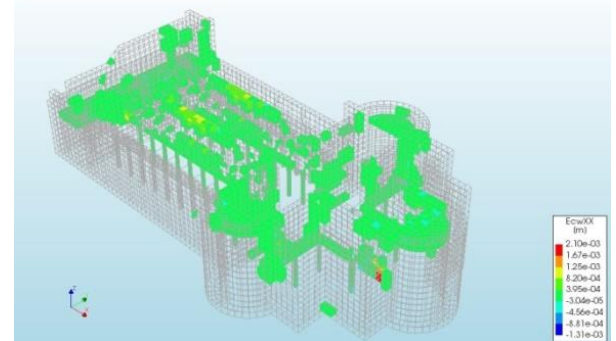
Load Step (13) : Crack width 2.17 mm

Analysis_20190330_X
Load-step 14, Load-factor 0.24602, Pushover_X
Crack-widths EcwXX
min: -1.27e-03m max: 2.10e-03m



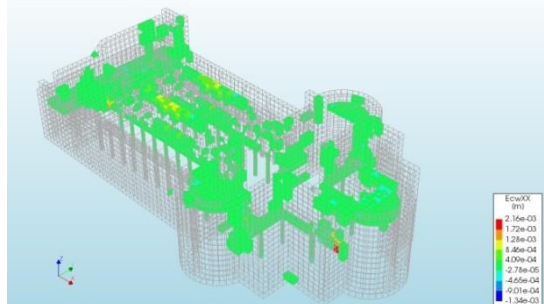
Load Step (14) : Crack width 2.10 mm

Analysis_20190330_X
Load-step 15, Load-factor 0.27543, Pushover_X
Crack-widths EcwXX
min: -1.31e-03m max: 2.10e-03m



Load Step (15) : Crack width 2.10 mm

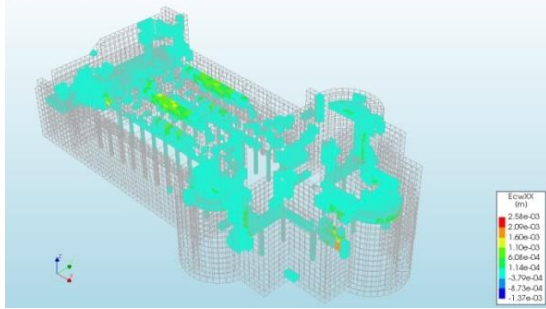
Analysis_20190330_X
Load-step 16, Load-factor 0.29395, Pushover_X
Crack-widths EcwXX
min: -1.34e-03m max: 2.16e-03m



Load Step (16) : Crack width 2.16 mm

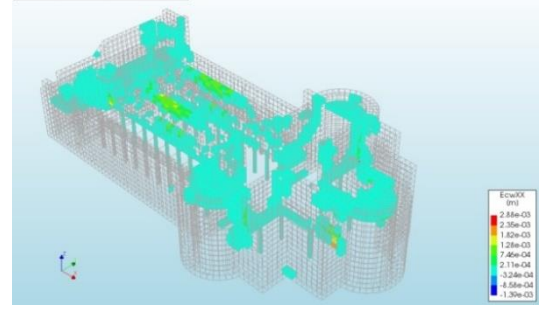
Fig. 14 Continued

Analysis_20190330_X
Load-step 17, Load-factor 0.30268, Pushover_X
Crack-widths EcwXX
min: -1.33e-03m max: 2.58e-03m



Load Step (17) : Crack width 2.58 mm

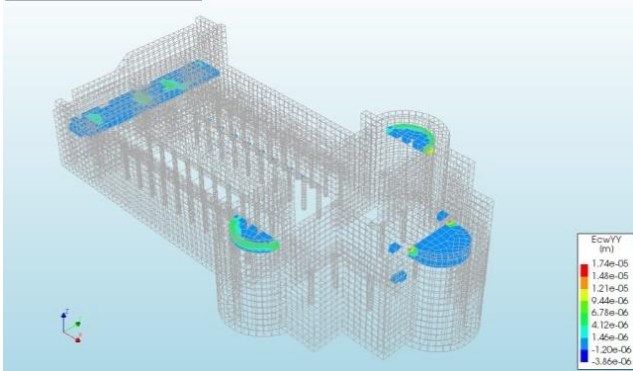
Analysis_20190330_X
Load-step 18, Load-factor 0.30274, Pushover_X
Crack-widths EcwXX
min: -1.39e-03m max: 2.88e-03m



Load Step (18) : Crack width 2.88 mm

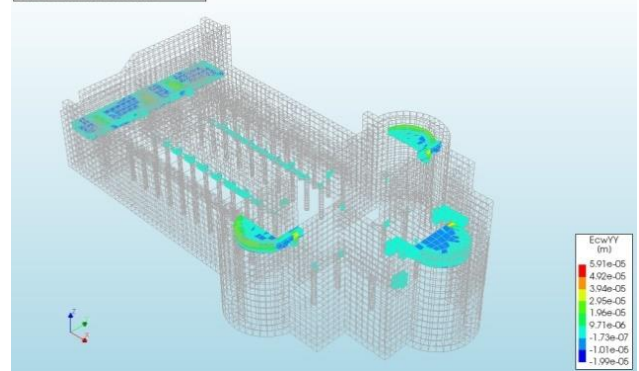
Fig. 14 Crack widths generated by pushover analysis in X - Direction

Analysis_20190330_Y
Load-step 1, Load-factor 0.19961, Self Load
Crack-widths EcwYY
min: -3.86e-05m max: 1.74e-05m



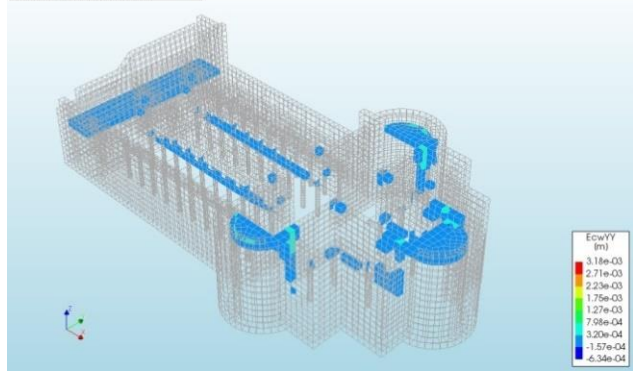
Load Step (1) : Crack width 0.017 mm

Analysis_20190330_Y
Load-step 2, Load-factor 0.39656, Self Load
Crack-widths EcwYY
min: -1.95e-05m max: 5.91e-05m



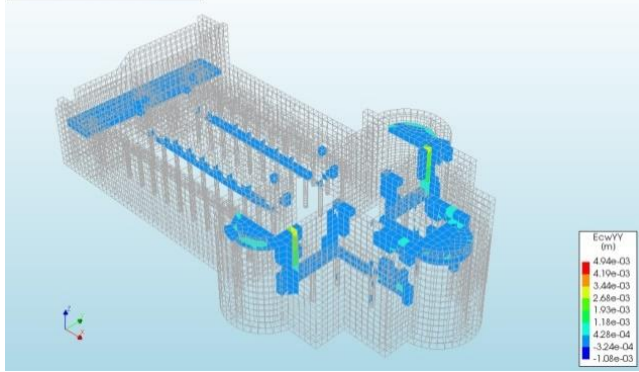
Load Step (2) : Crack width 0.059 mm

Analysis_20190330_Y
Load-step 3, Load-factor 0.48763, Self Load
Crack-widths EcwYY
min: -6.34e-04m max: 3.18e-03m



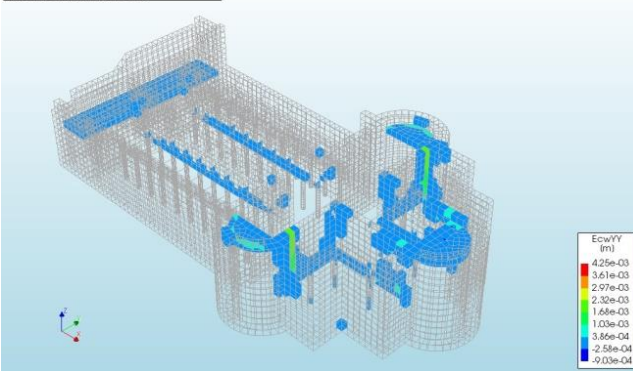
Load Step (3) : Crack width 3.18 mm

Analysis_20190330_Y
Load-step 4, Load-factor 0.111666, Self Load
Crack-widths EcwYY
min: -1.08e-03m max: 4.94e-03m



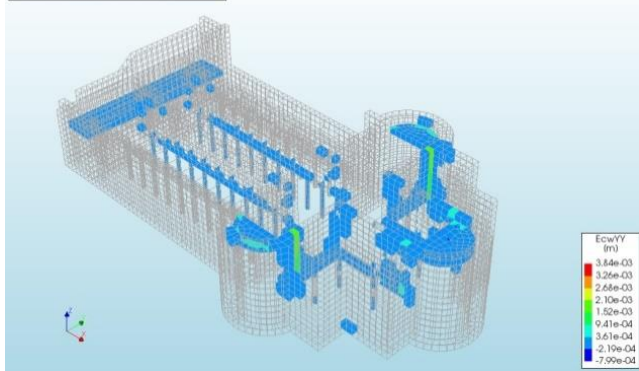
Load Step (4) : Crack width 4.94 mm

Analysis_20190330_Y
Load-step 5, Load-factor 0.14698E-01, Self Load
Crack-widths EcwYY
min: -9.03e-04m max: 4.25e-03m



Load Step (5) : Crack width 4.25 mm

Analysis_20190330_Y
Load-step 6, Load-factor 0.77710E-01, Self Load
Crack-widths EcwYY
min: -7.99e-04m max: 3.84e-03m



Load Step (6) : Crack width 3.84 mm

Fig. 15 Continued

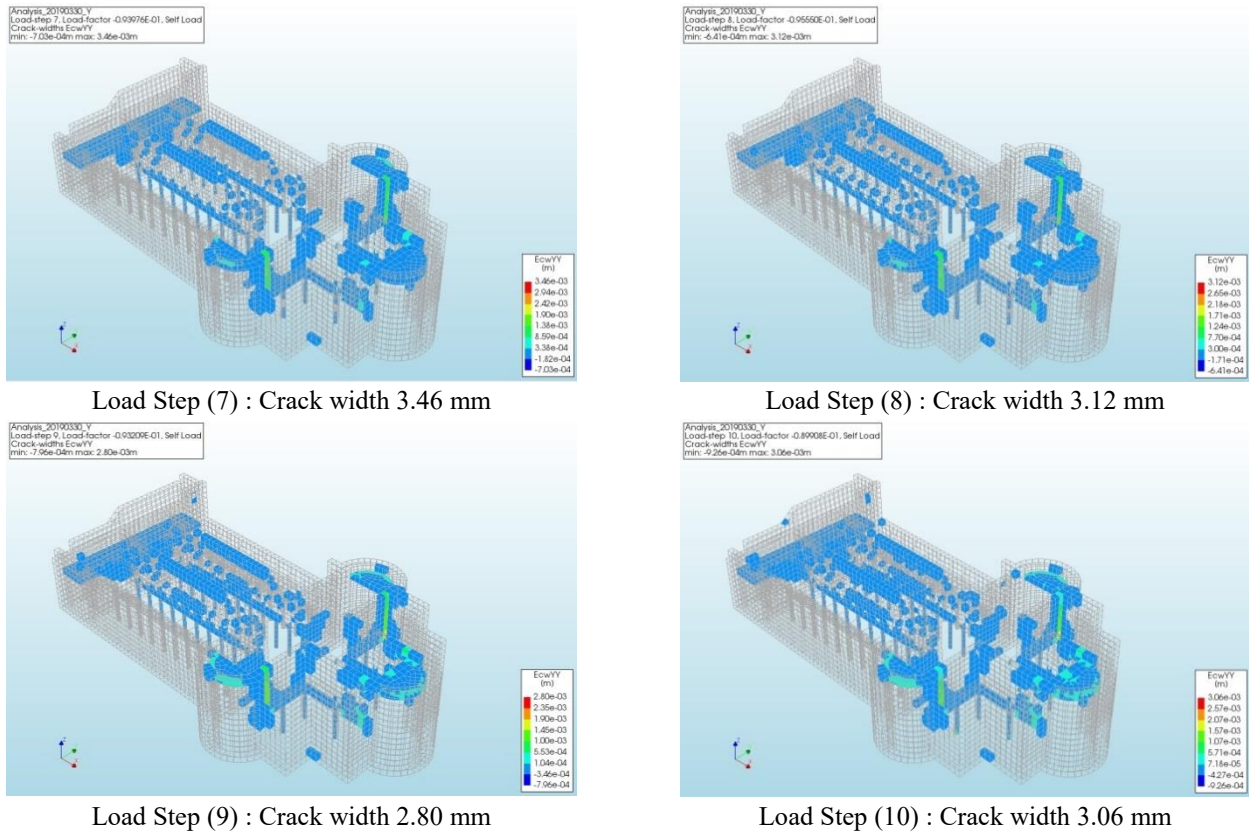


Fig. 15 Crack widths generated by gravity loads analysis in Y – Direction

significant cracks in gravity loads without any lateral load excitation, in detail, the contours show the values of cracks in some locations, concerning load steps of the self-load of the structure only, it's obvious that the cracks reached the max value of 5.97 mm in the vaults of the narthex, and the apses, shown in Fig. 13.

It is clear that the church components are coherent under gravity loads, suffering from a superficial deposit of atmospheric particulate, but the gross cracks generated from pushover excitations have to be monitored and require an assessment of the structural soundness of the elements. For this purpose, the model of Nativity Church which used as a damage monitoring method to check the crack stability and integrity state of elements was also used for the determination of cracks after the application of lateral loads, as shown in Fig. 14. The results showed that the masonry building is subjected to partially collapse during nonlinear static monotonic load, due to the loss of equilibrium of masonry portions, and enlargement of cracks widths as shown from load step (11) to load step (20). Expected local mechanisms that are generated from the analysis are essential issues in the seismic analysis of masonry buildings.

4.2 Cracks in Y – Direction

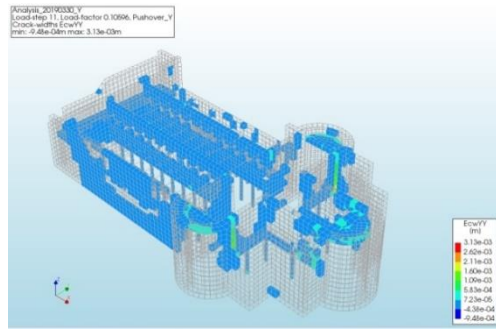
In the other direction Y, the damage propagation generated as a result of gravity load is symmetrical around the longitudinal east-west axis, as shown in Fig. 15. most cracks are situated above the narthex vaults, the apses vault

also propagates in the bottom parts of the lateral walls of the nave and shoulders of the church (premier walls). Generally, the structure presented a global damage behavior in the Y direction, without evident damage causing localized failures, the counters also show the values of cracks in some locations with reference to the load steps for the self-load, it's obvious that the cracks reached a maximum value of 4.94 mm in the vaults of the narthex, and the apses.

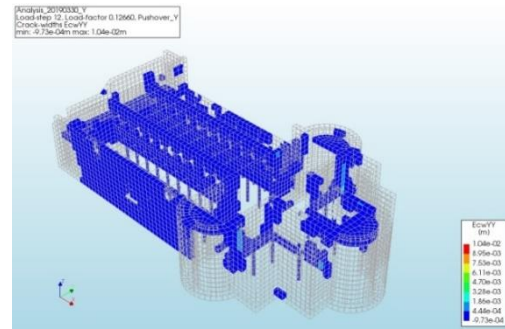
One of the benefits of using the pushover analysis tool, the out-of-plane behavior, can also be investigated. It is rather difficult to suggest detailed or realistic out-of-plane mechanisms, but the excitations of lateral loads, verified and shown in Fig. 16 has a width of 13.7 mm.

The out-of-plane movement is the most dangerous in this case, the vertical cracks on the connection between frontal and lateral facades indicate the activation of the façade overturning and the formation of hinges. The main structural causes of this mechanism are the weak connection with the orthogonal walls (90° walls), poor masonry quality, no box behavior, and the absence of links on the top, these results allow the researchers to verify the possibility of collapse caused by the plasticization of the material.

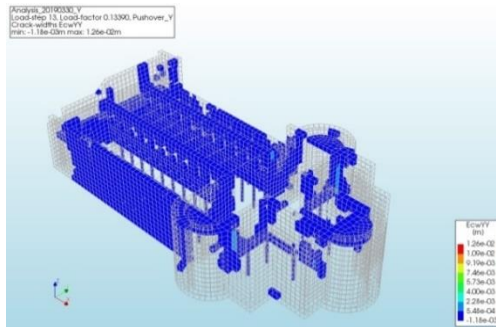
The pushover analysis results showed two types of local mechanisms in the Nativity Church, in-plane direction, and out-of-plane direction. The first type of mechanism has more stiffness than the second one, which presents the comparison between the maximum crack propagation in each direction concerning the load step, the maximum crack width generated in X- direction approximately remains



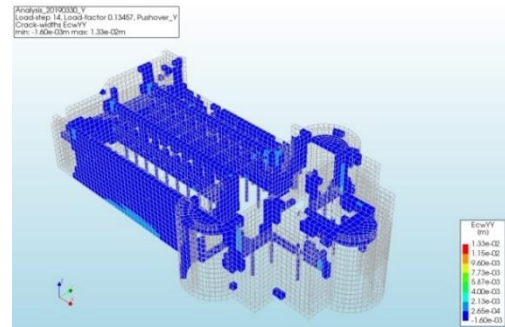
Load Step (11) : Crack width 3.13 mm



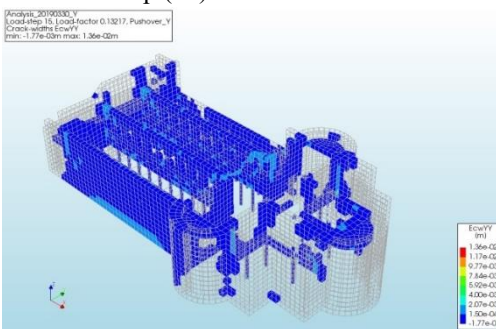
Load Step (12) : Crack width 10.4 mm



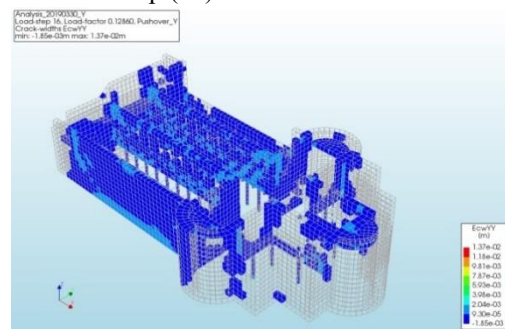
Load Step (13) : Crack width 12.6 mm



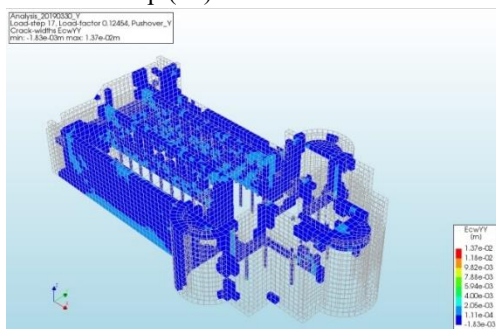
Load Step (14) : Crack width 13.3 mm



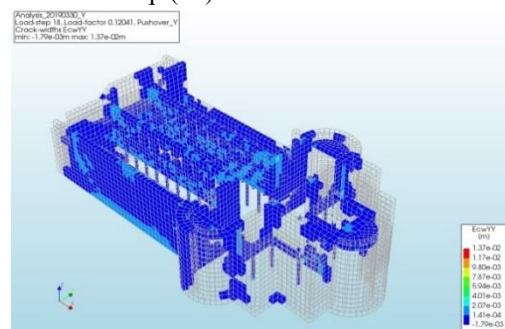
Load Step (15) : Crack width 13.6 mm



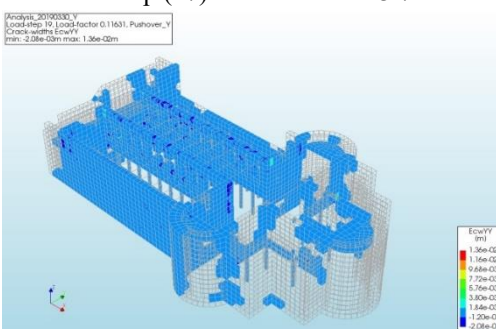
Load Step (16) : Crack width 13.7 mm



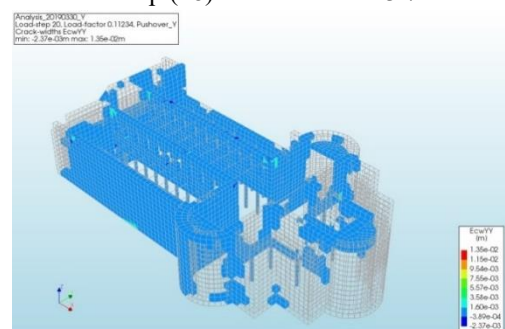
Load Step (17) : Crack width 13.7 mm



Load Step (18) : Crack width 13.7 mm



Load Step (19) : Crack width 13.6 mm



Load Step (20) : Crack width 13.5 mm

Fig. 16 Crack widths generated by pushover analysis in Y – Direction

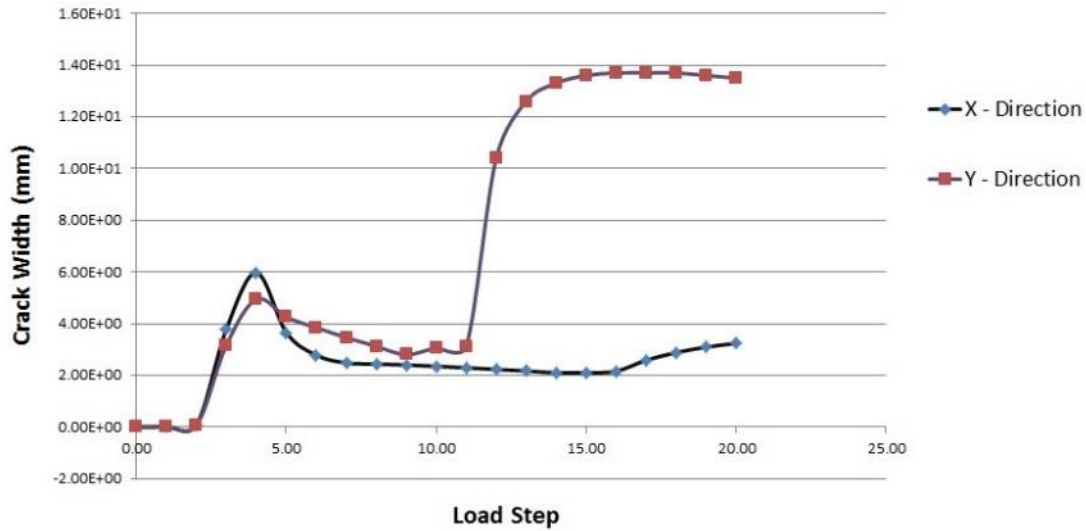


Fig. 17 Maximum crack propagation in each direction with respect to load step

Table 4 Maximum crack width in X Vs. Y directions

| Elements of Church | X – Direction (In-plane) | | Y – Direction (Out-of-Plane) | |
|------------------------|--------------------------|--------------|------------------------------|--------------|
| | Crack width | Crack length | Crack width | Crack length |
| Façade | 3.24 mm | Continuous | 13.7 mm | Continuous |
| buttress | ~ Zero | ~ Zero | ~ Zero | ~ Zero |
| Columns | 3.24 mm | Continuous | 13.7 mm | Continuous |
| Exterior Lateral Walls | ~ Zero | Zero | 13.7 mm | Continuous |
| Interior Lateral Walls | 3.24 mm | Continuous | 13.7 mm | Continuous |
| Transverse Walls | 3.24 mm | Continuous | 13.7 mm | Continuous |
| Side ApSES | ~ Zero | ~ Zero | 13.7 mm | Continuous |
| Central Apse | ~ Zero | ~ Zero | ~ Zero | ~ Zero |
| Shoulders | ~ Zero | ~ Zero | ~ Zero | ~ Zero |
| Vaults | 3.24 mm | Continuous | 13.7 mm | Continuous |

slightly small with a modest difference, this is evident by examining the points before the load step (10), which refer to gravity loads excitations, and after load step (10) which refer to the pushover excitations. For example, the load step (9), has a crack width of 2.40 mm, and for the load step (11), the crack width was 2.29 mm, which means that the difference was 5%.

(Alessandri and Turrioni 2018) found that it's obvious that crack propagation is reliable in the investigation of the historical masonry structures, as not only the bandwidth of cracks is checked, but also the length of cracks can be checked and investigated, and give a good indication of what will happen for seismic loads. On another hand, the out-of-plane stiffness of the church is lower than in-plane stiffness, the Y direction was more deformed and had a larger crack width, numerically, the maximum crack width before load step (10), i.e., load step (9) was 2.80 mm, and after the load step (10), i.e., load step (12), was 10.40 mm. Fig. 17 also presents the jump between the two directions.

To determine the limit state, and according to the IBC 2015 – (2109.3.1.4) “The Shrinkage cracks in adobe units shall not contain more than three shrinkage cracks and any single shrinkage crack shall not exceed 3 inches (76 mm) in length or 1/8 inch (3.2 mm) in width”. The researchers

decided to make the limit state of (the values larger than shrinkage cracks are critical and must be given high attention and good treatment), the decision will be that; crack propagations indicates there is a large problem in out-of-plane direction (Y – direction), but still at the upper limit in the in-plane direction (X – direction), in more details, Y – direction, exceeds the limits in width and length with a maximum width of 13.7 mm (approximately more than 400% of the values considered in the IBC 2015 as shrinkage crack), also in length of cracks, they are continues with each other (no specified length). Otherwise, X – direction is failed in length but still at most width, with no ignoring to the problem of a lot of cracks. Table 4 summarizes the results of crack details for each structural element of the church.

4.3 Critical Region Identification results

Based on the dynamic analysis, the following results can be discussed, based on the failure criteria. The von misses stress exceeds the limiting value of shear stress that the masonry walls resist, this leads to collapse of blocks at certain region after 7.53 seconds of analysis. it's important to show the damping ratio which are presented in Fig. 18.

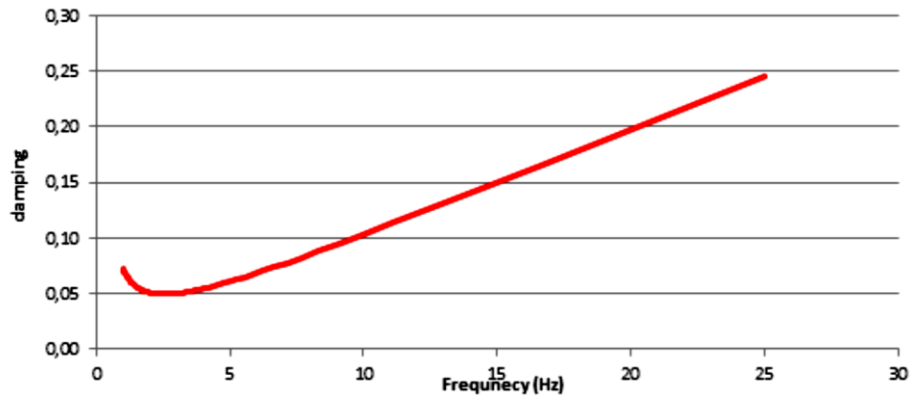


Fig. 18 Rayleigh Damping Model

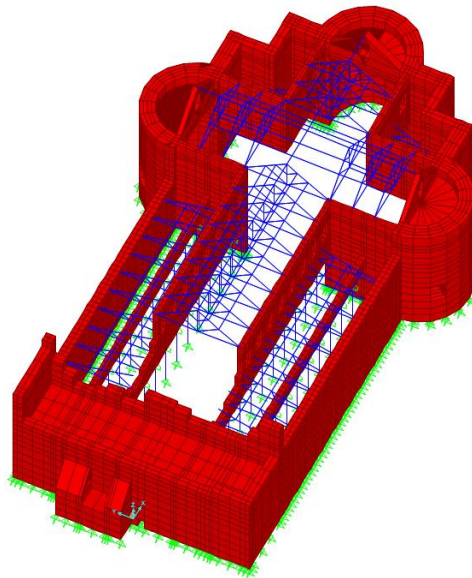


Fig. 19 Facade overturning failure after 7.53 sec

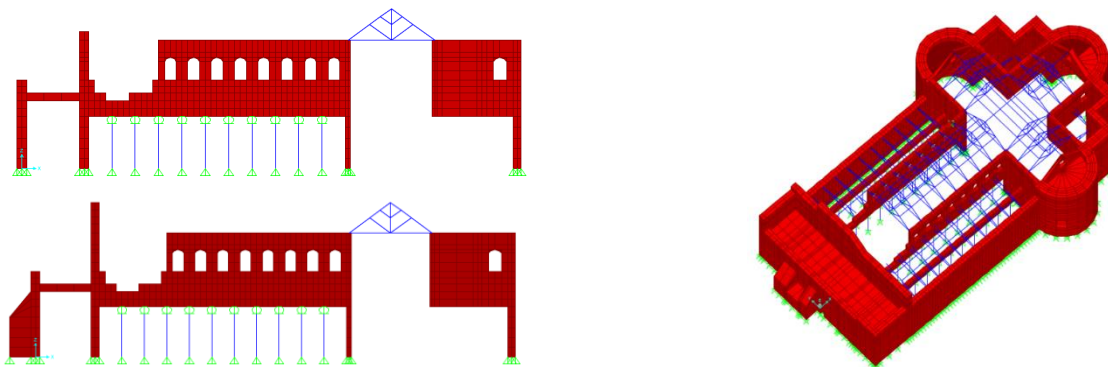


Fig. 20 Lateral walls failure after 7.53 sec

For the evaluation of the progressive collapse in each direction, the same control points adopted in the pushover are considered.

The first failure, summarized in the mechanism regarding the narthex overturning, and the loss of connection in the lateral walls connected to façade, the maximum von misses' results is 125.00 KN/m² which exceeds the upper limit 89 KN/m², so each element in the

structure treated individually and the area collapse is shown in Fig. 20.

As a second stage, after 7.53 seconds, Fig. 20 shows the detached areas. Surly the building is not fit enough to prevent the excitation as well as expected.

Before going on to the Y direction, the results checked again for the rest duration (between 7.53 sec to 39.09 sec) to ensure that there are no other failed areas. This means

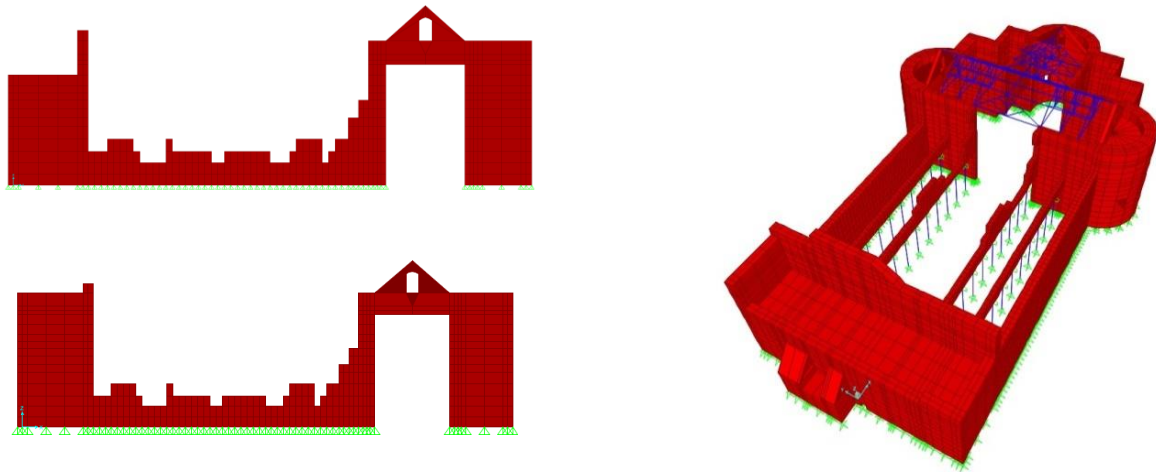


Fig. 21 External and internal lateral walls failure

Table 5 Effect of Progressive Collapse Analysis

| Elements of Church | X - Direction | Y - Direction |
|------------------------|---------------------------------|---------------------------------|
| Façade | Collapsed Progressively | Doesn't Collapsed Progressively |
| Buttress | Doesn't Collapsed Progressively | Doesn't Collapsed Progressively |
| Columns | Doesn't Collapsed Progressively | Doesn't Collapsed Progressively |
| Exterior Lateral Walls | Doesn't Collapsed Progressively | Collapsed Progressively |
| Interior Lateral Walls | Collapsed Progressively | Collapsed Progressively |
| Transverse Walls | Doesn't Collapsed Progressively | Doesn't Collapsed Progressively |
| Side Apses | Doesn't Collapsed Progressively | Doesn't Collapsed Progressively |
| Central Apse | Doesn't Collapsed Progressively | Doesn't Collapsed Progressively |
| Shoulders | Doesn't Collapsed Progressively | Doesn't Collapsed Progressively |
| Vaults | Doesn't Collapsed Progressively | Doesn't Collapsed Progressively |

that in plane behavior of church suffering only from narthex disruptive motion and detachment between the connections between members of walls and façade.

As done in the X direction, the rest of earthquake excitation (between 7.53 sec to 39.09 sec) shows no more failed elements, so we can summarize that in out of plane orientation of entire structure, the relatively long walls are the critical element, add to that, the trusses that lies on these walls will collapse, with the upper roof of church carried on, which means almost complete collapse for the mosaic panels on walls, see Fig. 21.

The Heritage constructions pose the largest challenges to the engineering researches, due to the limited knowledge of the existing structure and the difficulty to improve the knowledge without compromising the preservation of the assets.

Provisions of existing codes inadequate to capture the uncertainty of the analysis of historic churches, or any historical structure, also the lack of reference values of critical variables from literature, and the limitations of carrying out tests to measure these critical variables, results in levels of uncertainty larger than the typical uncertainty of the assessment of existing buildings made of modern materials. Moreover, existing codes and guidelines for assessment of existing constructions ignore the fact mentioned in this thesis that decisions made by the analyst during the analysis and definition of actions contribute to the overall uncertainty as much as other aspects, such as the

geometry, materials and structural details of the heritage construction. The most critical aspect of the modeling is simulation of the response of stone masonry by appropriate constitutive model. Under earthquake loading, thick walls and buttresses respond mainly in shear, with a low tensile strength and brittle response.

The comprehensive evaluation process of progressive collapse includes the aspects related to building layout, i.e., investigation of geometrical information, material properties, structural constructions etc. The development of all kinds of detection techniques will help to improve the objectivity and accuracy of the evaluation for structures to resist progressive collapse. Based on the finite element simulation, the study replicated the collapse process and evaluated the importance indices of all the structural elements, the limit used was by application of the modified von misses failure criterion, the stresses at reference nodes are calculated and compared to the permissible values of the stresses generated by the model and taken by von misses criterion must not exceed 0.089 MPa for Perimeter walls, 0.067 MPa for specific narthex components, and 0.02 MPa for vaults. Based on these results of progressive collapse, reliable and simple identification method of the critical regions was proposed. The identified critical regions can be used to facilitate a rational design, construction, inspection and maintenance practice, which would thereby lead to prevention strategies and minimize the likelihood of any failure. Table 5 shows the elements of church which are

failed in shear.

5. Conclusions

A numerical simulation procedure employing pushover analysis predicting the seismic behavior of the nativity church has been proposed in this study, the crack propagation was observed in both x and y directions, and the following points can be concluded:

- The results showed that the masonry building is subjected to partial collapses in many locations during nonlinear static monotonic load, due to the loss of equilibrium of masonry portions and enlargement of crack widths.
- The pushover analysis showed that the seismic performance of the Nativity church was dependent on its critical transversal Y-direction, it had more deformation and larger crack width than in X-direction.
- The out-of-plane movement (Y-direction) is the most dangerous case, the vertical cracks on the connection between frontal and lateral facades indicate the activation of the façade overturning and the formation of hinges.
- Crack width was at the upper limit in the in-plane direction (X – direction). While, in Y – direction, it exceeded the limits of IBC code in width and length with a maximum width of 13.7 mm.
- The modal analysis indicated frequencies ranging from 1.82 Hz to 5.56 Hz of the first eight modes of vibration for the structure. These modes possess cumulative mass participation above 70% in both orthogonal directions (X and Y directions). The comparison of the numerical frequencies and mode shapes, made for the first eight modes of vibration, resulted in a significant variation of the frequencies with a maximum error of 11.23%
- A nonlinear dynamic analysis is recommended in the near future for the Nativity church, which takes into account the materials nonlinearity.
- In smeared crack approach, it has always been implicitly understood that the criterion for the onset of cracking, which is always established in terms of stresses and strains, so the researcher should also automatically define the direction of propagation, and this is a natural assumption in the continuum problem, with proper evaluation of stress and strain values and directions.

References

- Alessandri, C. and Turrioni, J. (2018), “The church of the nativity in Bethlehem: Analysis of a local structural consolidation”, *Int. J. Civil Eng.*, **16**(5), 457-474. <https://doi.org/10.1007/s40999-017-0148-0>.
- Artar, M., Coban, K., Yurdakul, M., Can, O., Yilmaz, F. and Yildiz, M.B. (2019), “Investigation on seismic isolation retrofit of a historical masonry structure”, *Earthq. Struct.*, **16**(4), 501-512. <https://doi.org/10.12989/EAS.2019.16.4.501>.
- Betti, M. and Vignoli, A. (2008), “Assessment of seismic resistance of a basilica-type church under earthquake loading: Modeling and analysis”, *Advan. Eng. Software*, **39**(4), 258-283. <https://doi.org/10.1016/j.advengsoft.2007.01.004>.
- Chalioris, C.E., Tsioukas, V.E., Favvata, M.J and Karayannis, C.G. (2013), “Recording historic masonry buildings using photogrammetry-two case studies”, *InCOMPADYN: Proceedings of the 4th international conference on computational methods in structural dynamics and earthquake engineering, Kos Island, Greece*.
- Dogangun, A. and Sezen, H. (2012), “Seismic vulnerability and preservation of historical masonry monumental structures”, *Earthq. Struct.*, **3**(1), 83-95. <https://doi.org/10.12989/eas.2012.3.1.083>.
- Fajfar, P. (2000), “A nonlinear analysis method for performance-based seismic design”, *Earthq. Spectra*, **16**(3), 573-592. <https://doi.org/10.1193/1.1586128>.
- Hadzima-Nyarko, M., Ademovic, N., Pavic, G. and Sipos, T.K. (2018), “Strengthening techniques for masonry structures of cultural heritage according to recent Croatian provisions”, *Earthq. Struct.*, **15**(5), 473-485. <https://doi.org/10.12989/EAS.2018.15.5.473>.
- Hadzima-Nyarko, M., Pavić, G. and Lešić, M. (2016), “Seismic vulnerability of old confined masonry buildings in Osijek, Croatia”, *Earthq. Struct.*, **11**(4), 629-648. <https://doi.org/10.12989/eas.2016.11.4.629>.
- IBC (2015), *International Building Code*. International Building Council, Inc.
- Kalkbrenner, P., Pelà, L., and Sandoval, C. (2019), “Multi directional pushover analysis of irregular masonry buildings without box behavior”, *Eng. Struct.*, **201**, 109534. <https://doi.org/10.1016/j.engstruct.2019.109534>.
- Karantoni, F., Tsionis, G., Lyrantzaki, F. and Fardis. M.N. (2014), “Seismic fragility of regular masonry buildings for in-plane and out-of-plane failure”, *Earthq. Struct.*, **6**(6), 689-713. <https://doi.org/10.12989/eas.2014.6.6.689>.
- Karantoni, F.V. (2013), “Seismic retrofitting of Fragavilla Monastery”, *Earthq. Struct.*, **5**(2), 207-223. <https://doi.org/10.12989/eas.2013.5.2.207>.
- Kouris, E.G., Kouris, L.A., Konstantinidis, A.A., Karayannis, C.G. and Aifantis, E.C. (2021), “Assessment and fragility of Byzantine unreinforced masonry towers”. *Infrastruct.*, **6**(3), 40. <https://doi.org/10.3390/infrastructures6030040>.
- Lagomarsino, S. (2006), “On the vulnerability assessment of monumental buildings”, *Bull. Earthq. Eng.*, **4**(4), 445-463. <https://doi.org/10.1007/s10518-006-9025-y>.
- Lourenço, P.B. (2002), “Computations on historic masonry structures”, *Progress Struct. Eng. Mater.*, **4**(3), 301-319. <https://doi.org/10.1002/pse.120>.
- Lourenço, P.B., Mendes, N., Ramos, L.F. and Oliveira, D.V. (2011), “Analysis of masonry structures without box behavior”, *Int. J. Architect. Heritage*, **5**(4-5), 369-382. <https://doi.org/10.1080/15583058.2010.528824>.
- Lourenço, P.B., Roque, J.C.A and Oliveira, D.V. (2012), “Seismic safety assessment of the Church of Monastery of Jeronimos, Portugal”, *15th International Brick and Block Masonry Conference*, Florianópolis, Santa Caterina, Brazil, June. <http://hdl.handle.net/1822/21477>.
- Magenes, G. (2000), “A method for pushover analysis in seismic assessment of masonry buildings”, *In Proceedings of The 12th World Conference On Earthquake Engineering*, Auckland, New Zeland, January.
- Milani, G. and Valente, M. (2015a), “Comparative pushover and limit analyses on seven masonry churches damaged by the 2012 Emilia-Romagna (Italy) seismic events: Possibilities of non-linear finite elements compared with pre-assigned failure mechanisms”, *Eng. Fail. Analy.*, **47** (PartA), 129-161. <https://doi.org/10.1016/j.engfailanal.2014.09.016>.
- Milani, G. and Valente, M. (2015b), “Failure analysis of seven

- masonry churches severely damaged during the 2012 Emilia-Romagna (Italy) earthquake: Non-linear dynamic analyses vs conventional static approaches”, *Eng. Fail. Anal.*, **54**, 13-56. <https://doi.org/10.1016/j.engfailanal.2015.03.016>.
- Milani, G., Valente, M. and Alessandri, C. (2016), “Nativity church in Bethlehem: Full 3D non-linear FE approach for structural damage prediction”, In *ECCOMAS-VII European Congress on Computational Methods in Applied Sciences and Engineering*, Crete, Greece, June. <http://hdl.handle.net/11392/2358799>.
- Moratti, M., Gaia, F., Martini, S., Tsioli, C., Grecchi, G., Casotto, C., Calvi, G.M., Den Hertog, D., Calvi, P.M. and Proestos, G.T. (2019), “A methodology for the seismic multilevel assessment of unreinforced masonry church inventories in the Groningen area”, *Bull. Earthq. Eng.*, **17**(8), 4625-4650. <https://doi.org/10.1007/s10518-019-00575-7>.
- Noel, M.F., Moreira, S., Briceño, C., López-Hurtado, E. and Aguilar, R. (2019), “Seismic assessment of the Church of San Sebastian in Cusco, Peru by means of pushover nonlinear analysis”, *Struct. Anal. Historic. Construct.*, **18**, 1462-1470. https://doi.org/10.1007/978-3-319-99441-3_157.
- Palacio, K. (2013), “Practical recommendations for nonlinear structural analysis in DIANA”. *TNO DIANA BV, Delft*.
- Ramírez, R., Mendes, N. and Lourenço, P.B. (2019), “Diagnosis and seismic behavior evaluation of the Church of São Miguel de Refojos (Portugal)”, *Build.*, **9**(6), 138. <https://doi.org/10.3390/buildings9060138>.
- Ranjbaran, F. and Hosseini, M. (2014), “Seismic vulnerability assessment of confined masonry wall buildings”, *Earthq. Struct.*, **7**(2), 201-216. <https://doi.org/10.12989/eas.2014.7.2.201>.
- Reyes, J.C. and Chopra, A.K. (2012), “Modal pushover-based scaling of two components of ground motion records for nonlinear RHA of structures”, *Earthq. Spectra*, **28**(3), 1243-1267. <https://doi.org/10.1193/1.4000069>.
- Roque, J., Oliveira, D.V., Ferreira, T.M. and Lourenço, P.B. (2019), “Nonlinear dynamic analysis for safety assessment of heritage buildings: Church of Santa Maria de Belém”, *J. Struct. Eng.*, **145**(12), 04019153. [https://doi.org/10.1061/\(ASCE\)ST.1943-541X.0002437](https://doi.org/10.1061/(ASCE)ST.1943-541X.0002437).
- Rossi, M., Calderini, C., Roselli, I., Mongelli, M., De Canio, G. and Lagomarsino, S. (2020), “Seismic analysis of a masonry cross vault through shaking table tests: the case study of the Dey Mosque in Algiers”, *Earthq. Struct.*, **18**(1), 57-72. <https://doi.org/10.12989/EAS.2020.18.1.057>.
- Shomali, Q. (2003), “Church of the Nativity: History & structure”, In *Proceedings of the International Congress More than Two Thousand Years in the History of Architecture*, UNESCO, Paris, December.
- Soulis, V.J. and Manos, G.C. (2019), “Numerical simulation and failure analysis of St. Konstantinos Church, after the Kozani Earthquake”, *Int. J. Civil Eng.*, **17**(7), 949-967. <https://doi.org/10.1007/s40999-018-0345-5>.
- Tezcan, S., Tambe, N., Muir, C., Aguilar, R. and Perucchio, R. (2019), “Nonlinear FE analysis of the response to lateral accelerations of the triumphal arch of the Church of Andahuaylillas, Peru”, *Struct. Anal. Historic. Construct.*, **18**, 1301-1309. https://doi.org/10.1007/978-3-319-99441-3_139.
- Touqan, A.R. and Salawdeh, S. (2015), “Major steps needed towards earthquake resistant design”, In *The 6 Jordanian International Civil Engineering Conference (JICEC06)*, Amman, March.
- Tsonos, A.G. (2007), “Effectiveness of CFRP jackets in post-earthquake and pre-earthquake retrofitting of beam-column subassemblages”, *Struct. Eng. Mech.*, **27**(4), 393-408. <https://doi.org/10.1016/j.engstruct.2007.05.008>.
- Tzanakis, M.J., Papagiannopoulos, G.A. and Hatzigeorgiou, G.D. (2016), “Seismic response and retrofitting proposals of the St. Titus Church, Heraklion, Crete, Greece”, *Earthq. Struct.*, **10**(6), 1347-1367. <https://doi.org/10.12989/eas.2016.10.6.1347>.
- Ural, A. (2017), “Masonry building behaviors during the February 6-12, 2017 Ayvacik-Çanakkale Earthquakes”, *Earthq. Struct.*, **17**(4), 355-363. <https://doi.org/10.12989/EAS.2019.17.4.355>.

AT